XIXth Workshop on High Energy Spin Physics dedicated to 90th anniversary of A.V. Efremov birth

Transition energy crossing of polarized proton beam at NICA.

Speaker: Kolokolchikov S. [1,2] (sergey.bell13@gmail.com)

Co-authors: Senichev Yu. [1,2], Aksentev A. [1,2,3], Melnikov A. [1,2,4]

[1]Institute for Nuclear Research RAS, Moscow, Russia,

[2]Moscow Institute of Physics and Technology, Dolgoprudny, Russia,

[3]Moscow Engineering Physics Institute (MEPI), Moscow

[4]Landau Institute for Theoretical Physics, Chernogolovka,

JOINT INSTITUTE FOR NUCLEAR RESEARCH

Dubna, 04 September 2023.

Abstract

At an experiment on acceleration of a polarized proton beam up to an energy at 13 GeV, the possibility of crossing the transition energy at 5.7 GeV by a jump is considered.

The scheme of crossing by a rapid change of transition energy, assumes the longitudinal movement of the beam near the zero value of the slip coefficient.

The jump itself is carried out in the absence of an RF field. The paper presents the influence of the above features on the dynamics of a polarized beam.

TABLE OF CONTENTS

Transition Energy

Momentum compaction factor at Transition

Energy change → 1) momentum change; 2) trajectory change.

	MCF	Slip-factor	
1st Ord	$\alpha = \frac{d\,C/C}{d\,p/p}$	$\eta = -\frac{\Delta\,f/f}{\Delta\,p/p}$	$\eta = \alpha - \frac{1}{\gamma^2}$
2nd Ord	$\frac{\Delta C}{C_0} = \alpha_0\delta + \alpha_1\delta^2 + \cdots$	$\frac{\Delta f}{f_0} = \eta_0\delta + \eta_1\delta^2 + \cdots$	$\eta_0 = \alpha_0 - \frac{1}{\gamma^2}$ $\eta_1 = \alpha_1 - \frac{\eta_0}{\gamma^2} + \frac{3\beta^2}{2\gamma^2}$

At $\eta = 0$ get for Lorentz-factor $\gamma_{\text{кр}} = \frac{1}{\sqrt{\alpha}}$, thus, transition energy can be determine.

Equations of Longitudinal Motion

Classical form

$$\frac{d\tau}{dt} = \eta \cdot \frac{h \cdot \Delta E}{\beta^2 \cdot E_0}$$

$$\frac{d(\Delta E)}{dt} = \frac{V(\tau)}{T_0}$$

	Variables
Normalised tracking	$\phi,\ \dot{\phi}$
Time- and energy offset based	$\Delta t, \Delta E$
Phase and relative momentum offset based	$\phi,\ \delta = \Delta p/p$

Equations in program

$$\frac{d\tau}{dn} = \eta\left(\frac{dp}{p}\right) \cdot \frac{T_0 \cdot h \cdot \Delta E}{\beta^2 \cdot E_0}$$

$$\frac{d(\Delta E)}{dn} = V(\tau)$$

$$\Delta E^{n+1} = \Delta E^n + \sum_{k=0}^{n_{\text{rf}}-1} V_k^n \sin\varphi_{\text{rf},k}(\Delta t^n) - (E_s^{n+1} - E_s^n).$$ – Energy Kick

$$t^{n+1} = t^n + \frac{2\pi}{\omega^{n+1}},$$ – arrival Time drift

Slippage factor

$$\frac{\Delta\omega}{\omega_0} = \frac{\omega - \omega_0}{\omega_0} \equiv -\eta(\delta)\delta = -(\eta_0 + \eta_1\delta + \eta_2\delta^2 + \ldots)\delta,$$

$$\eta_0 = \alpha_0 - \frac{1}{\gamma_s^2} \qquad \eta_1 = \frac{3\beta_s^2}{2\gamma_s^2} + \alpha_1 - \alpha_0\eta_0$$

$$\eta_2 = -\frac{\beta_s^2(5\beta_s^2 - 1)}{2\gamma_s^2} + \alpha_2 - 2\alpha_0\alpha_1 + \frac{\alpha_1}{\gamma_s^2} + \alpha_0^2\eta_0 - \frac{3\beta_s^2\alpha_0}{2\gamma_s^2},$$

Synchronious Particle

$$\sum_{k=0}^{n_{\text{rf}}-1} V_k^n \sin\varphi_{\text{rf},k}(\Delta t_s^n) - e\int_{\Delta t_{\min}}^{\Delta t_s^n} d\tau\,\lambda(\tau)W(\Delta t_s^n - \tau) = (E_s^{n+1} - E_s^n),$$

BLonD: https://blond.web.cern.ch/

Coasting Beam

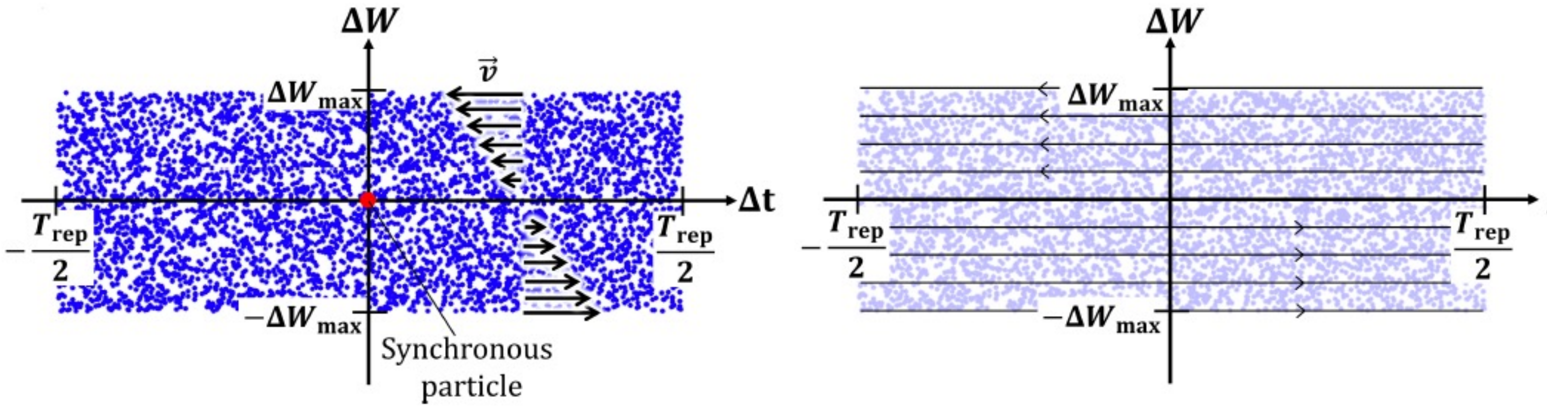

Figure 2.2: Phase space for a coasting beam (no gap voltages applied) below transition energy ($\eta_R > 1$). On the left, a number of particles which have been mapped to phase space can be seen. In addition, the movement of particles in phase space is visualized by black arrows according to the tracking equations in (2.7) and (2.8) with $\vec{v} = (0, \Delta W \cdot \text{const})$. On the right, the corresponding trajectories are shown. The particles are shown lightly to emphasize the connection between both phase space presentations.

Jens Schweickhardt, Modeling and Optimization of Barrier-Bucket RF Systems, 2021

Jump-scheme at NICA

$$\Delta n := n_{tr} - \frac{(\gamma_{tr} - \Delta\gamma_{tr} - 1)\cdot m_p - E_{inj}}{U} = 1.407 \times 10^5$$ – turns before jump

$$\Delta n_{jump} := \frac{2\Delta\gamma_{tr}}{T_s \cdot d\gamma dt} = 6.225 \times 10^3$$ – turns at jump

$$T_s \cdot d\gamma dt \cdot \Delta n_{jump} = 0.09$$ – $\Delta\gamma_{jump}$

$$T_s \cdot \Delta n_{jump} \cdot 10^3 = 10.588 \quad \text{ms}$$ – jump time

Here is a 5 different states of longitudinal optics based on **transition energy**:
1) acceleration from injection energy with initial value;
2) smooth increase to peak;
3) jump;
4) smooth recovery till initial transition;
5) initial value till the experiment energy;

1. First defines 3) state based on the maximum available speed of transition shift and available transition size
2. Secondly, we can understand states 3 and 4, as they changed parallel to beam energy
3. Finally, states 3 and 5 also can be understand

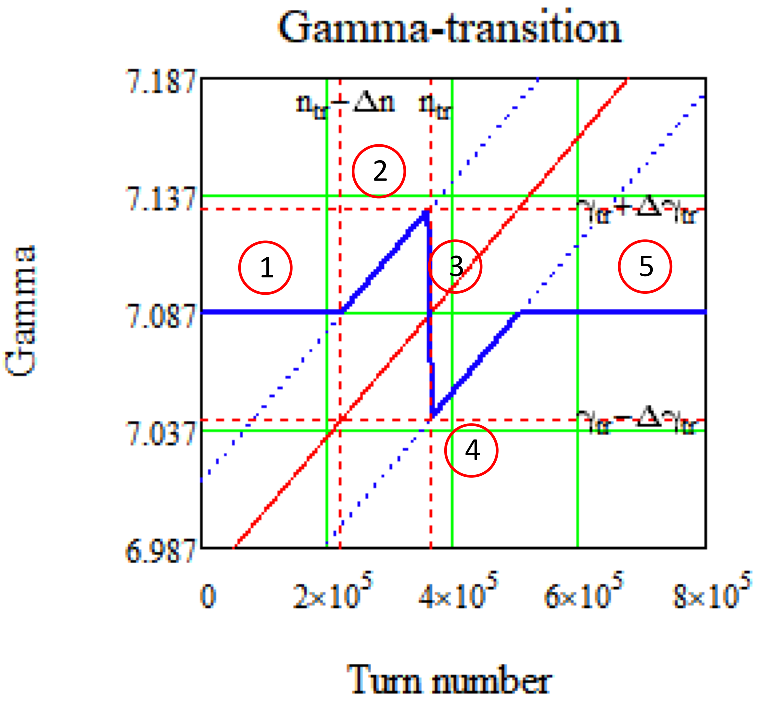

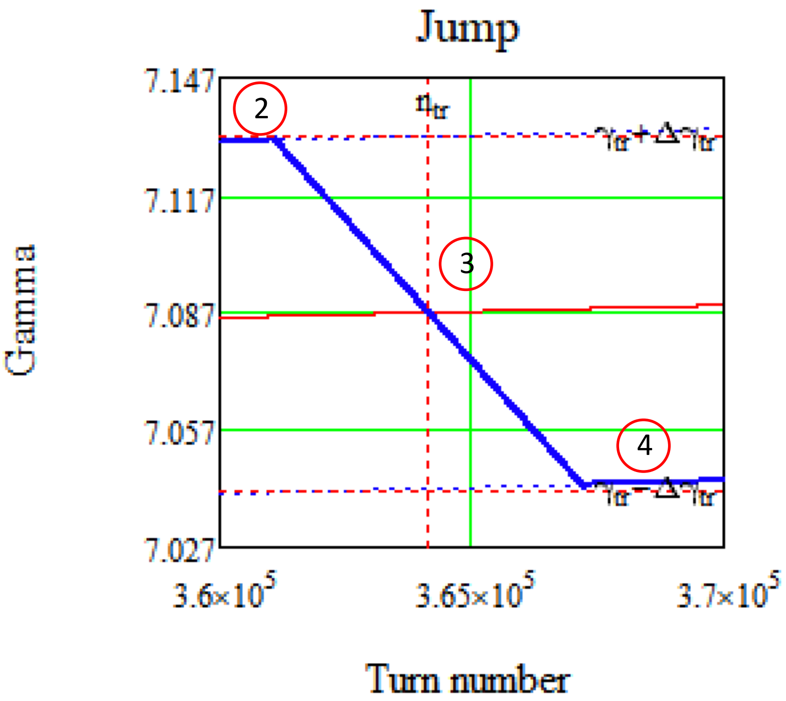

Momentum compaction factor at Transition

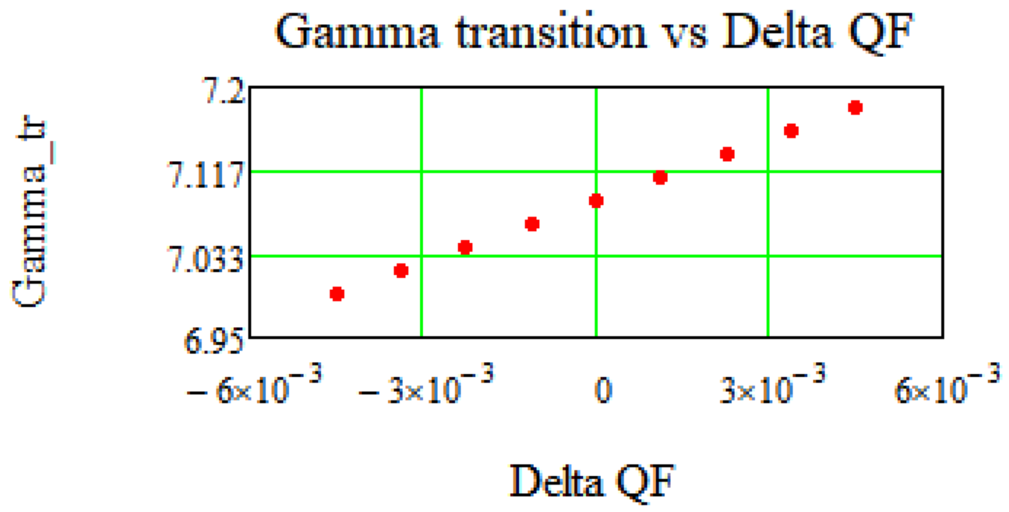

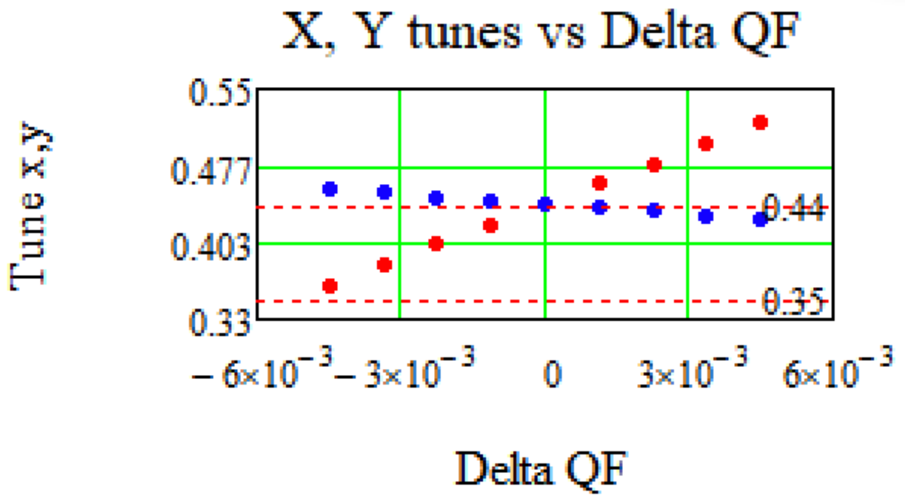

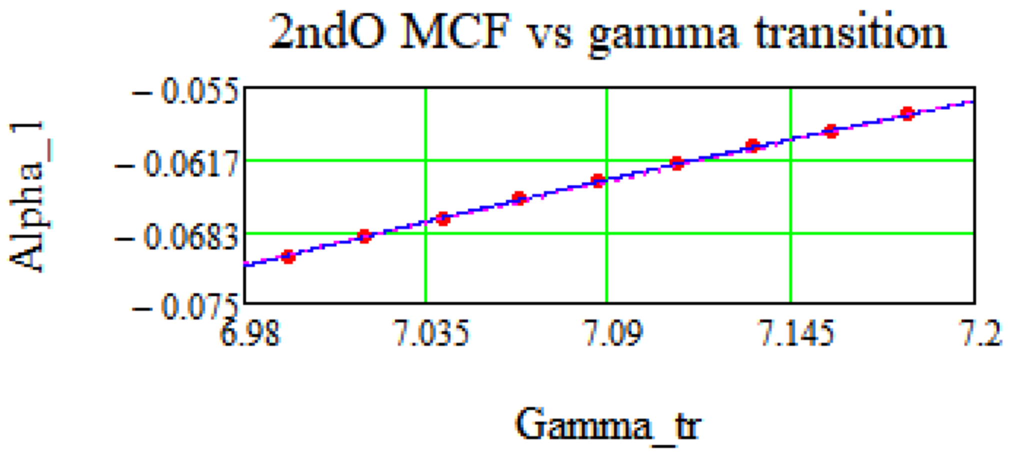

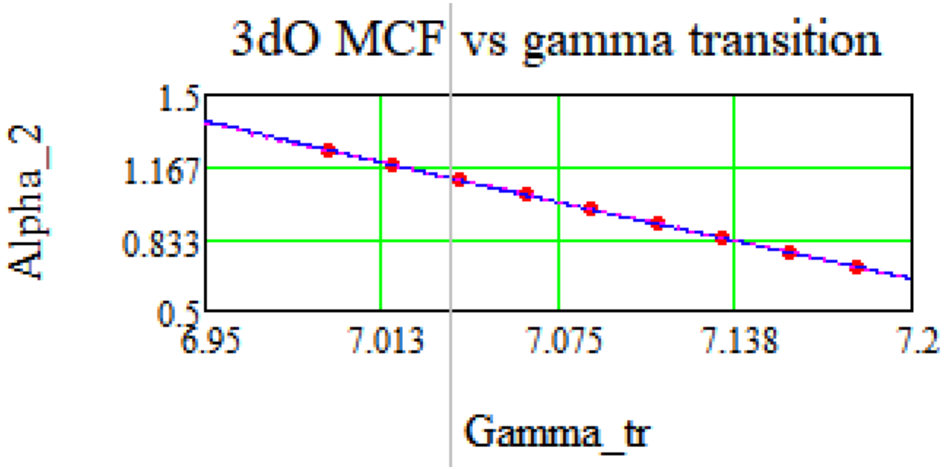

Dynamics aperture

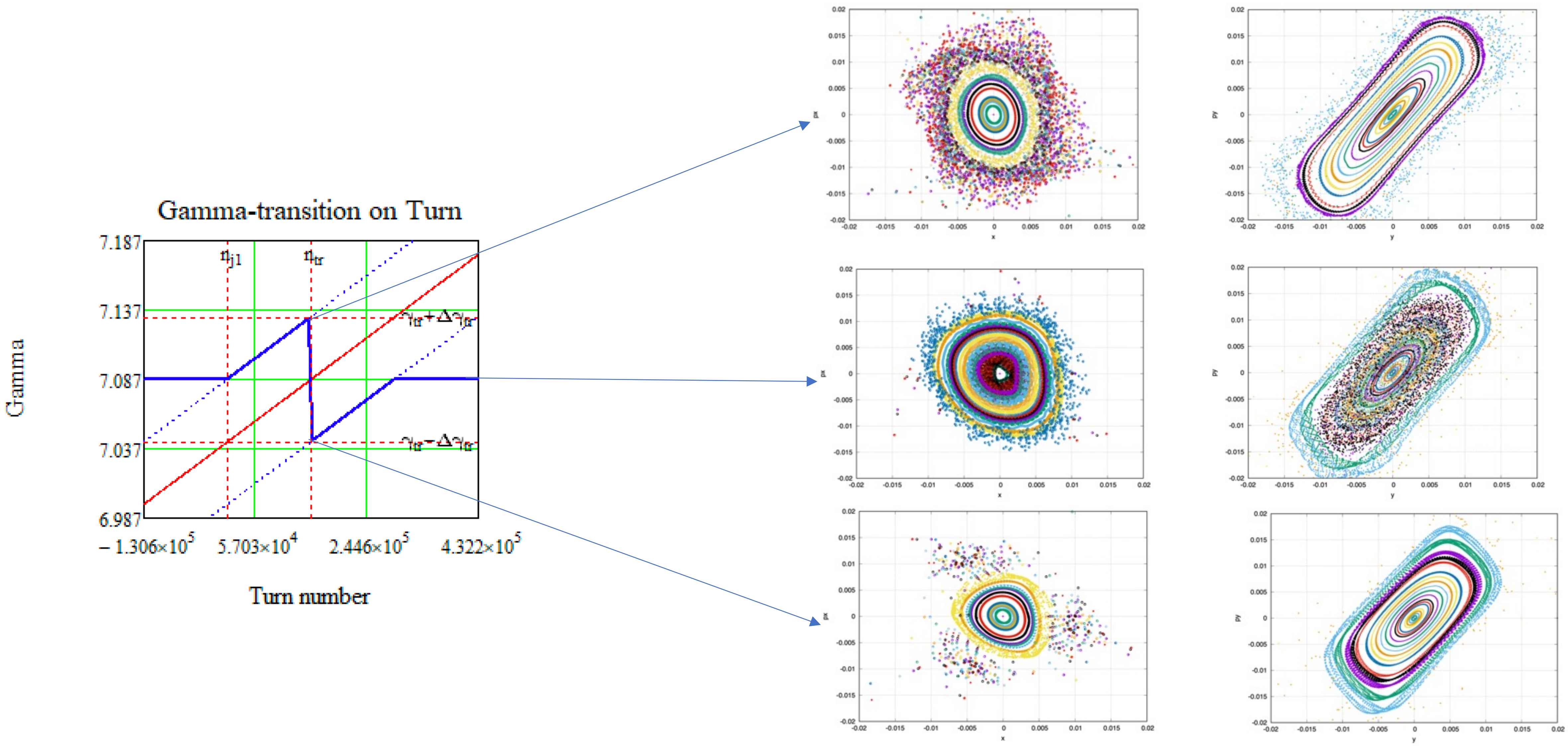

Impedance

NICA Elements

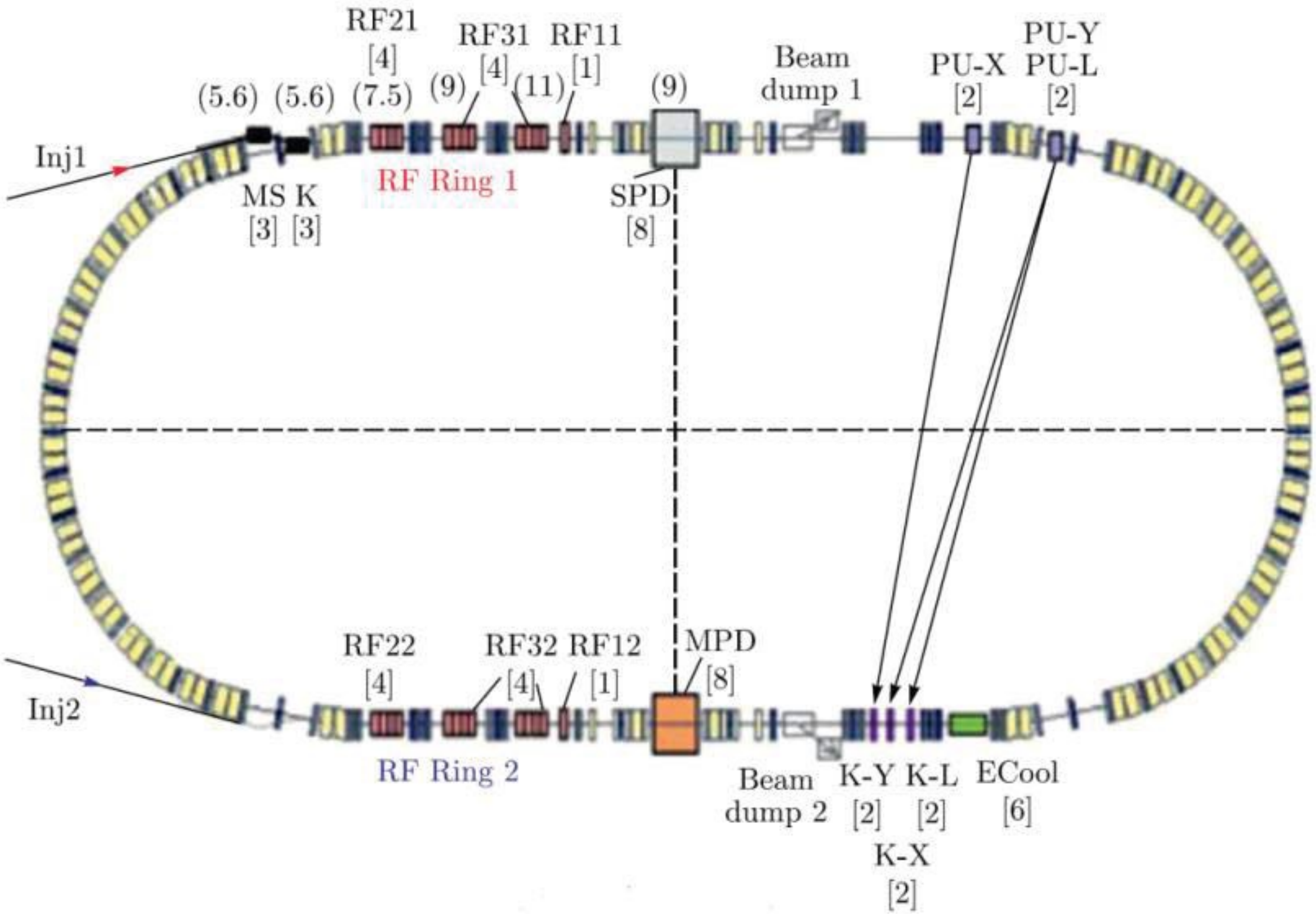

Impedances

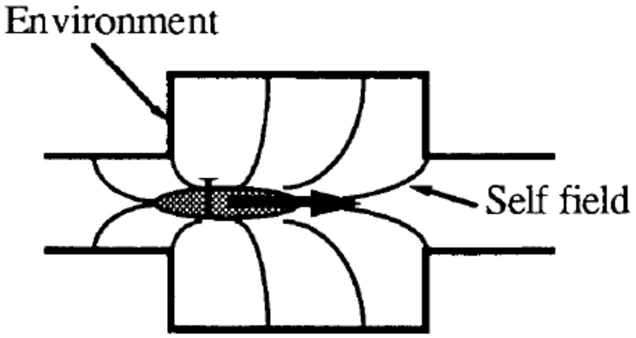

Fig. 1

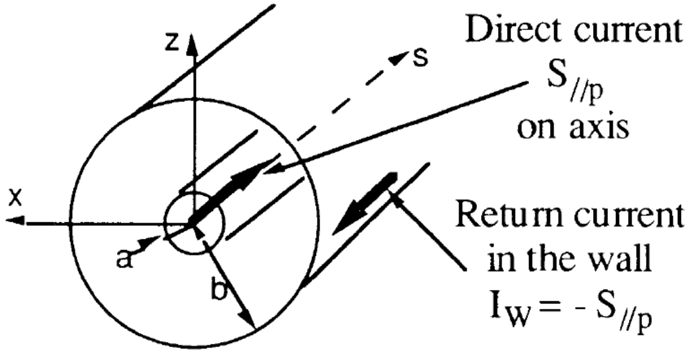

Laclare, J L (ESRF, Grenoble), Coasting beam longitudinal coherent instabilities, CAS - CERN Accelerator School : 5th General Accelerator Physics Course, pp.349-384, DOI: 10.5170/CERN-1994-001.349

Definition of Impedance:

$Z_{//}(\omega)$ is in fact a parameter which can only be drawn once Maxwell's equations have been completely solved. It gathers all the details of the electromagnetic coupling between the beam and the surroundings. By varying its form, we will be able to consider any type of beam self electromagnetic field.

To obtain a general mathematical expression, we introduce a distribution function: $\Psi(\tau,\dot{\tau},t)$ which represents the particle density in the bidimensional phase space and we write the signal of the entire beam:

$$S_{//}(t,\theta) = N\int_{\tau=0}^{\tau=T_0}\int_{\dot{\tau}=-\infty}^{\dot{\tau}=+\infty}\Psi(\tau,\dot{\tau},t)\,s_{//}(t,\theta)\,d\tau\, d\dot{\tau} \qquad (25)$$

Each individual frequency ω present in the Fourier transform of the signal contributes to the force and must be combined with the corresponding impedance at ω.

$$[\vec{E}+\vec{v}\times\vec{B}]_{//}(t,\theta)=\frac{-1}{2\pi R}\int_{\omega=-\infty}^{\omega=+\infty} Z_{//}(\omega)S_{//}(\omega,\theta)\exp j\omega t\, d\omega \qquad (57)$$

in which the following definitions are assumed.

Space Charge Impedance

$$\frac{Z}{n} = -\frac{Z_0[1+\log(\frac{b}{a})]}{2\beta\gamma^2}$$

$Z_{//}(\omega)$ but $\frac{Z_{//}(\omega)}{\omega}$ or $\frac{Z_{//}(\omega)}{p}$ with $p = \frac{\omega}{\omega_0}$

Space Charge Impedance

$Z_0 := 377 \quad \Omega \quad \text{Ohm}$ resistivity of free space

$a := 1.2$ cm beam size

$b := 2.86$ cm beam pipe radius

$C_{ring} = 503.04$

$c = 2.988 \times 10^8$

$$n_\sigma := \frac{b}{a}$$

$$Z_{SC}(\omega_{SC}, \gamma_{SC}) := -i \cdot \frac{Z_0}{2 \cdot \pi} \cdot \frac{\omega_{SC} \cdot C_{ring}}{\left(\gamma_{SC}^{\ 2} - 1\right) \cdot c} \cdot \ln\left(\frac{n_\sigma}{1.06}\right)$$

From V.Lebedev

$$Z_{SC}(n, \gamma_{SC}) := \frac{n \cdot Z_0}{2 \cdot \beta(\gamma_{SC}) \cdot \gamma_{SC}^{\ 2}} \cdot \left(1 + 2 \cdot \ln\left(\frac{b}{a}\right)\right)$$

Classical formula

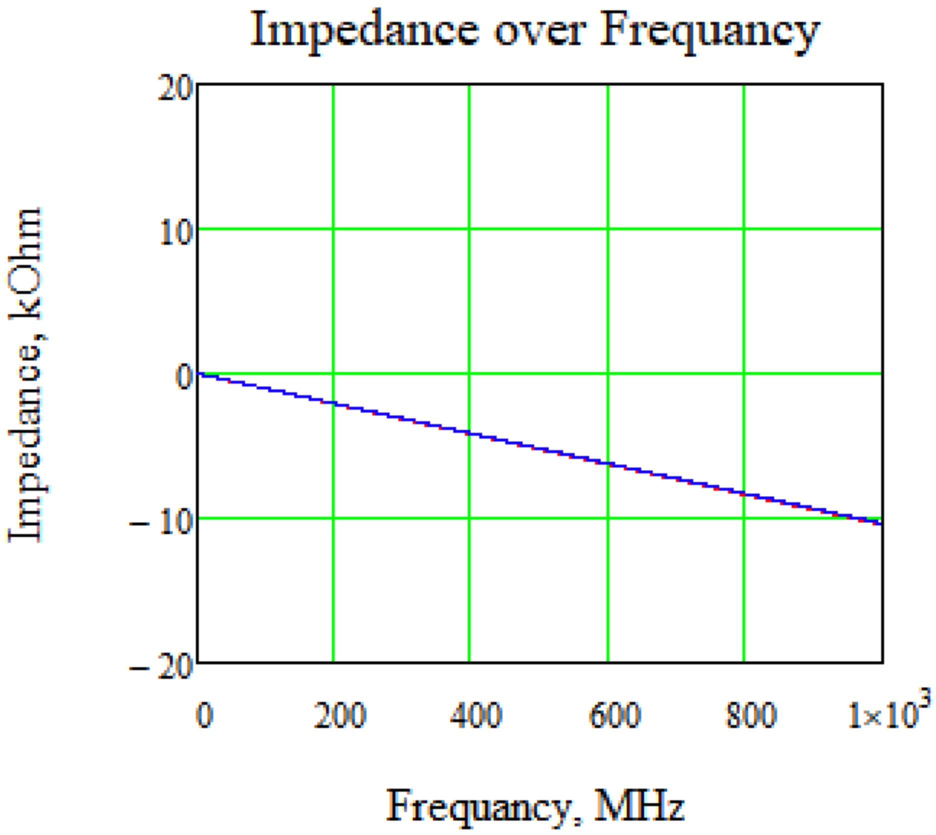

BLonD. Inductive Impedance (SC) – Induced Voltage

class `blond.impedances.impedance.InductiveImpedance`(*Beam, Profile, Z_over_n, RFParams, deriv_mode='gradient'*)

Bases: `blond.impedances.impedance._InducedVoltage`

Constant imaginary Z/n impedance

Parameters

- **Beam** (*object*) – Beam object
- **Profile** (*object*) – Profile object
- **Z_over_n** (*float array*) – Constant imaginary Z/n program in* Ω.
- **RFParams** (*object*) – RFStation object for turn counter and revolution period
- **deriv_mode** (*string, optional*) – Derivation method to compute induced voltage

class `blond.impedances.impedance.TotalInducedVoltage`(*Beam, Profile, induced_voltage_list*)

Bases: `object`

Object gathering all the induced voltage contributions. The input is a list of objects able to compute induced voltages (InducedVoltageTime, InducedVoltageFreq, InductiveImpedance). All the induced voltages will be summed in order to reduce the computing time. All the induced voltages should have the same slicing resolution.

Parameters

- **Beam** (*object*) – Beam object
- **Profile** (*object*) – Profile object
- **induced_voltage_list** (*object list*) – List of objects for which induced voltages have to be calculated

BLonD: https://blond.web.cern.ch/

P. F. Derwent, Implementation of BLonD for Booster Simulations, Beams-doc # 8690, 2020

Phase portraits of different BB

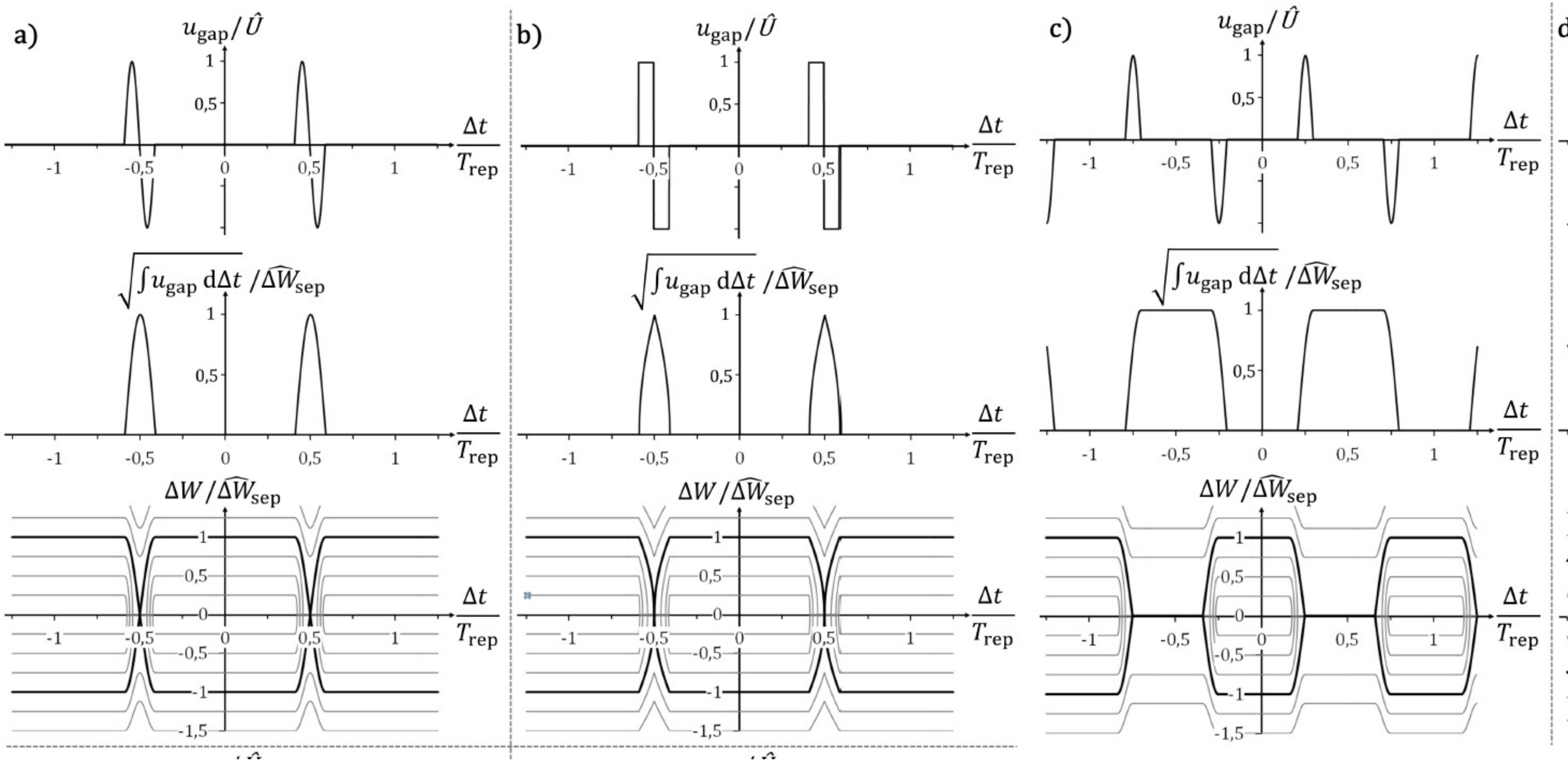

Jens Schweickhardt, Modeling and Optimization of Barrier-Bucket RF Systems, 2021

Figure 2.3: Phase portraits for different RF voltages and corresponding energy barriers: a) Single-sine voltage aimed for at the ESR, b) Rectangular barrier voltages as often used for theoretical considerations c) Barrier half waves creating flat potential plateaus, d) Harmonic gap voltage.

Fourier Expansion

Square signal

$$g(\phi) = \begin{cases} -\mathrm{sgn}(\eta), & \text{if } -\pi/h_\mathrm{r} \le \phi \le 0 \\ \mathrm{sgn}(\eta), & \text{if } 0 < \phi \le \pi/h_\mathrm{r} \\ 0, & \text{otherwise} . \end{cases} \quad (3.3)$$

Fourier Expansion

$$b_n = \mathrm{sgn}(\eta)\frac{2}{n\pi}\left[1 - \cos\left(\frac{n}{h_\mathrm{r}}\pi\right)\right] , \quad (3.4)$$

Sigma modulation

$$\sigma_m(n) = \mathrm{sinc}^m \frac{n\pi}{2(N+1)} , \quad (3.10)$$

$$V_n(t) = M_n \sin(n\omega t + \phi) . \quad (3.18)$$

$$M_n = \sigma(n) b(n,h) . \quad (3.19)$$

RF Kick

$$\Delta E_i' = \Delta E_i + \sum_{i=0}^{n_\mathrm{rf}-1} V_j \sin(\omega_j \Delta t_i + \phi_j) \quad (3.20)$$

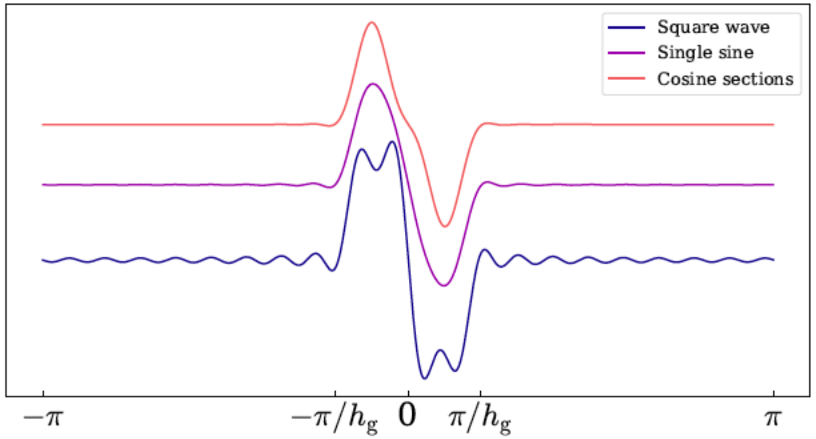

Figure 3.3: Comparison of different waveforms generated for the same gap width using 20 Fourier harmonics.

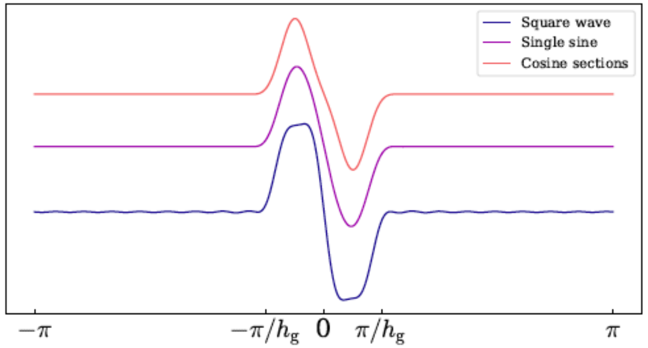

Figure 3.6: Comparison of different waveforms generated for the same gap width using 20 Fourier harmonics using σ_3 modulation.

Mihaly Vadai, Beam Loss Reduction by Barrier Buckets in the CERN Accelerator Complex, CERN, Geneva, 2021

Fourier expansion of Barrier Bucket

$\phi_r := \frac{2 \cdot T_1}{T_2} = 0.25$ Phase of Barrier gap

$h_r := \frac{\pi}{\phi_r} = 12.574$ BB harmonic number

$N := 25$ Fourier SUM

$$g_{BB}(\phi,\gamma,dp\_p) := -\mathrm{sign}(\eta(\gamma,dp\_p)) \cdot \left(\frac{-\pi}{h_r} \le \phi \le 0\right) + \mathrm{sign}(\eta(\gamma,dp\_p)) \cdot \left(0 < \phi \le \frac{\pi}{h_r}\right) + 0$$

$$b(n,h_r,\gamma,dp\_p) := \mathrm{sign}(\eta(\gamma,dp\_p)) \cdot \frac{2}{\pi n} \cdot \left(1 - \cos\left(\frac{\pi \cdot n}{h_r}\right)\right)$$ Fourier coefficients

$$\sigma(n,m) := \mathrm{sinc}\left[\frac{\pi \cdot n}{2(N+1)}\right]^m$$ Sigma modulation $\sigma(1,3) = 0.998$

$$g_{BB}(\phi,\gamma,dp\_p) := \sum_{n=1}^{N} \left(\sigma(n,3) \cdot b(n,h_r,\gamma,dp\_p) \cdot \sin(n \cdot \phi)\right)$$ Fourier signal of Square BB

$V_{peak} := 5000\ V$ (keV) $n_{rf} := 25$

$f(MHz) := MHz$ MHz

$\omega(i) := 2\pi \cdot f(i)$

$M(n,m,\gamma,dp\_p) := \sigma(n,m) \cdot b(n,h_r,\gamma,dp\_p)$

$$V_{BB}(\tau,\gamma,dp\_p) := \sum_{i=1}^{n_{rf}} \left[-V_{peak} \cdot [M(i,3,\gamma,dp\_p) \cdot \sin[(\omega(i)) \cdot \tau]]\right]$$

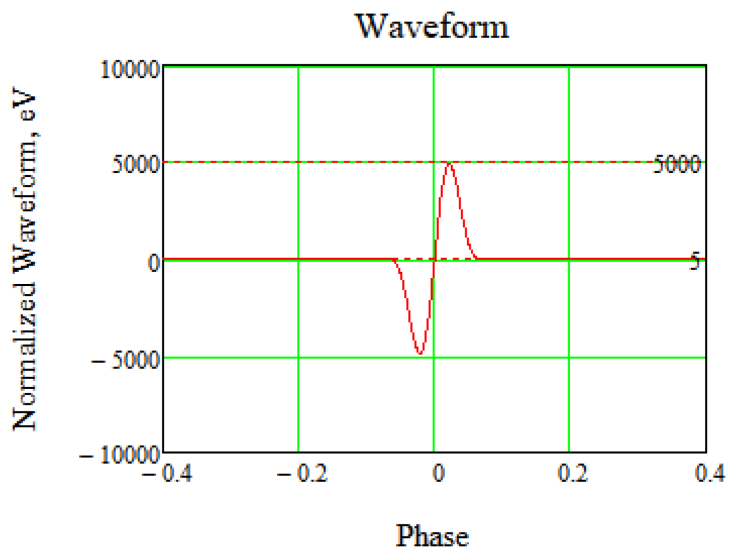

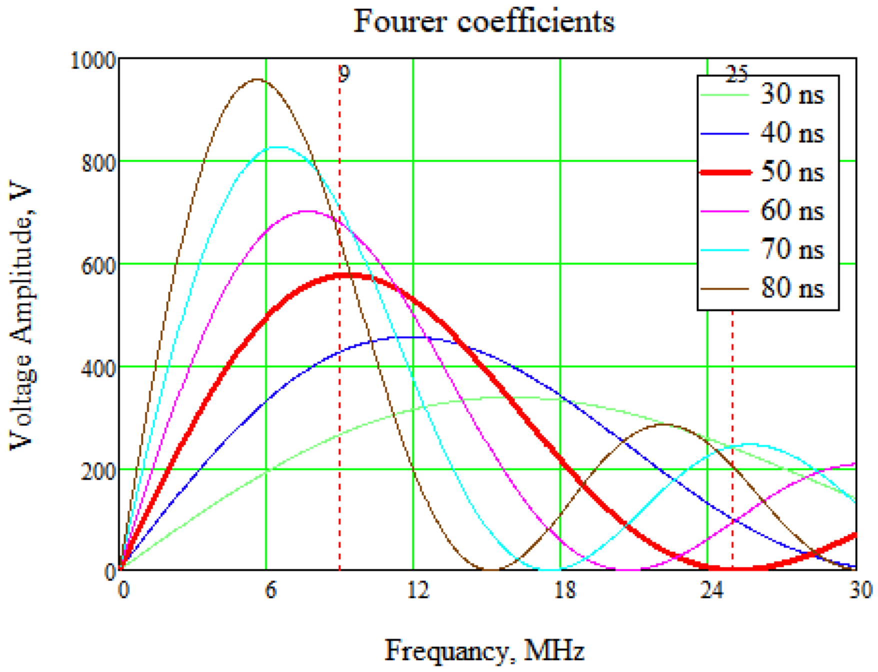

Separatrix of BB

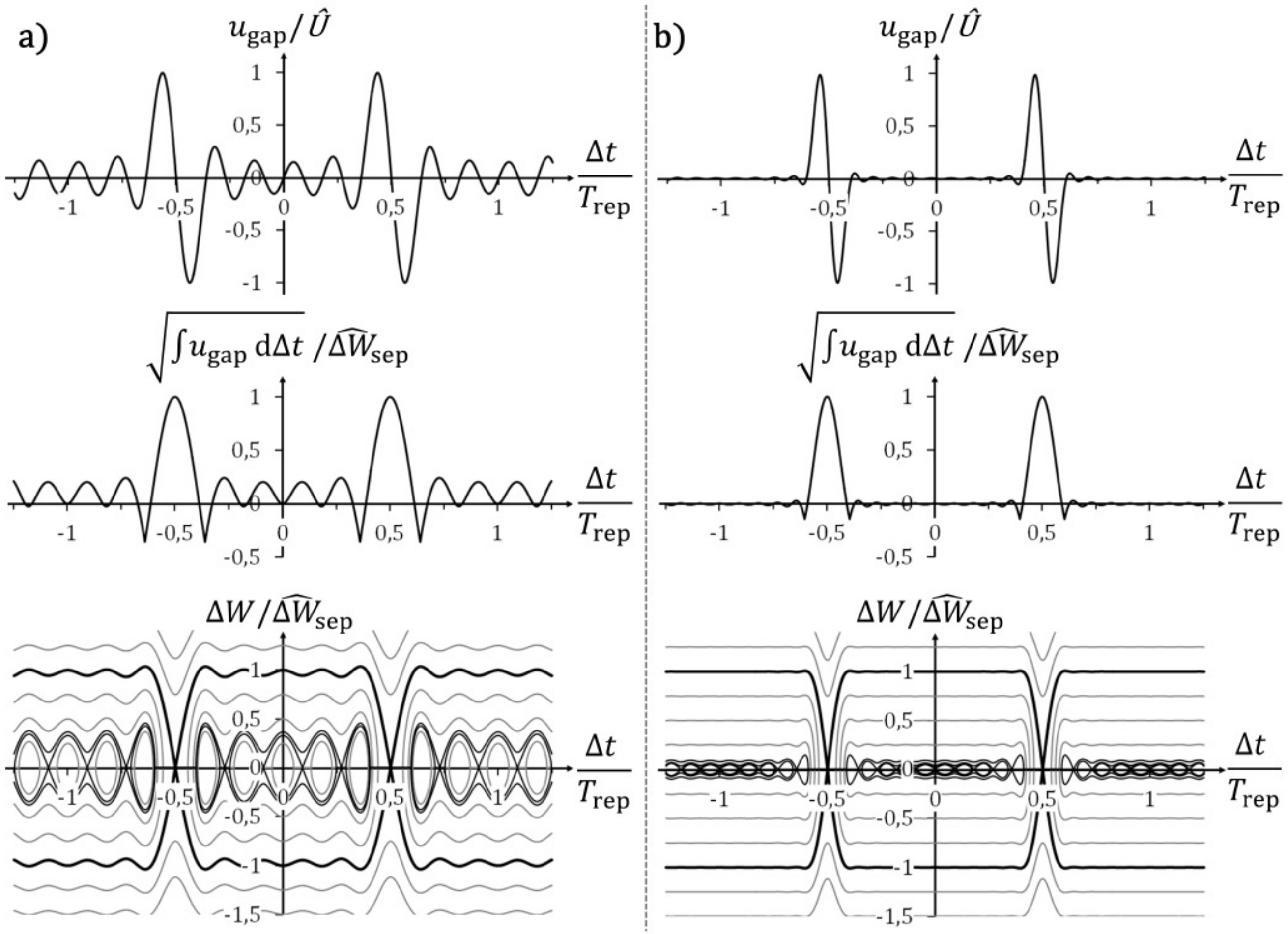

Figure 2.8: Phase portraits for BB signals with ringing between the pulses. For these signals, the ringing is caused by a limited bandwidth of a): $\omega_{max} = \omega_{BB}$ and b): $\omega_{max} = 2\omega_{BB}$. Trajectories are drawn in steps of $\frac{1}{4}\Delta W_{sep}$ in gray. Separatrices are drawn in black.

Jens Schweickhardt, Modeling and Optimization of Barrier-Bucket RF Systems, 2021

Orbital Tracking

Effect of High Order MCF

Kin. Energy, eV		Gamma	Momentum, eV/c	Total Energy, eV
$E_{kin}(n_{tr}) = 5.709 \times 10^9$	eV	$\gamma(n_{tr}) = 7.087$	$p(n_{tr}) = 6.581 \times 10^9$	$E_{beam}(n_{tr}) = 6.647 \times 10^9$
$E_{kin}(n_{tr} - \Delta n) = 5.667 \times 10^9$	eV	$\gamma(n_{tr} - \Delta n) = 7.042$	$p(n_{tr} - \Delta n) = 6.538 \times 10^9$	$E_{beam}(n_{tr} - \Delta n) = 6.605 \times 10^9$
$E_{kin}(n_{tr} + \Delta n) = 5.751 \times 10^9$	eV	$\gamma(n_{tr} + \Delta n) = 7.132$	$p(n_{tr} + \Delta n) = 6.623 \times 10^9$	$E_{beam}(n_{tr} + \Delta n) = 6.689 \times 10^9$

$E_{kin}(n_{tr} + \Delta n) - E_{kin}(n_{tr} - \Delta n) = 8.442 \times 10^7$ eV (84 MeV in) $2 \cdot \Delta n = 2.814 \times 10^5$ turns

- γ_{tr} – smooth increase (2nd stage)
- NO SC
- BB RF
- $\alpha_{0,1,2}$ stationary

At 2nd stage

$$\gamma_{tr} \parallel \gamma_{beam} \Rightarrow \eta_s \parallel \eta_{tr}$$
$$\eta_s = const$$

Taking into account $\delta = {}^{dp}/_{p}$,
get a range of η for different particles

Gamma-transition

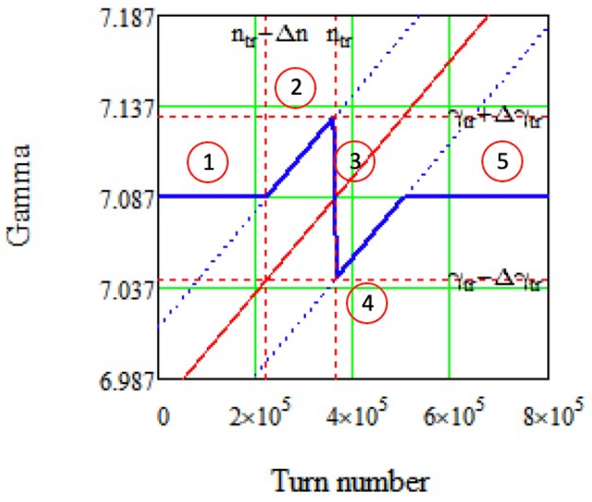

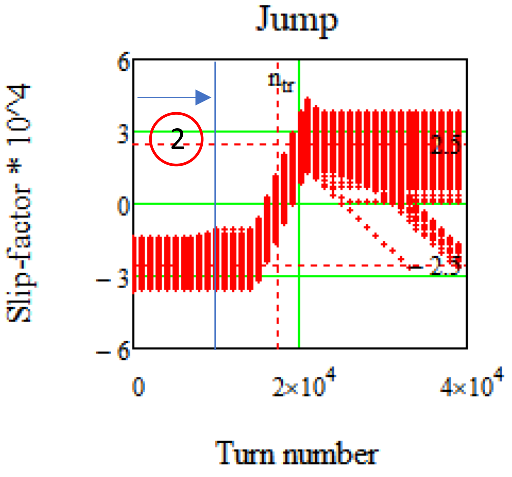

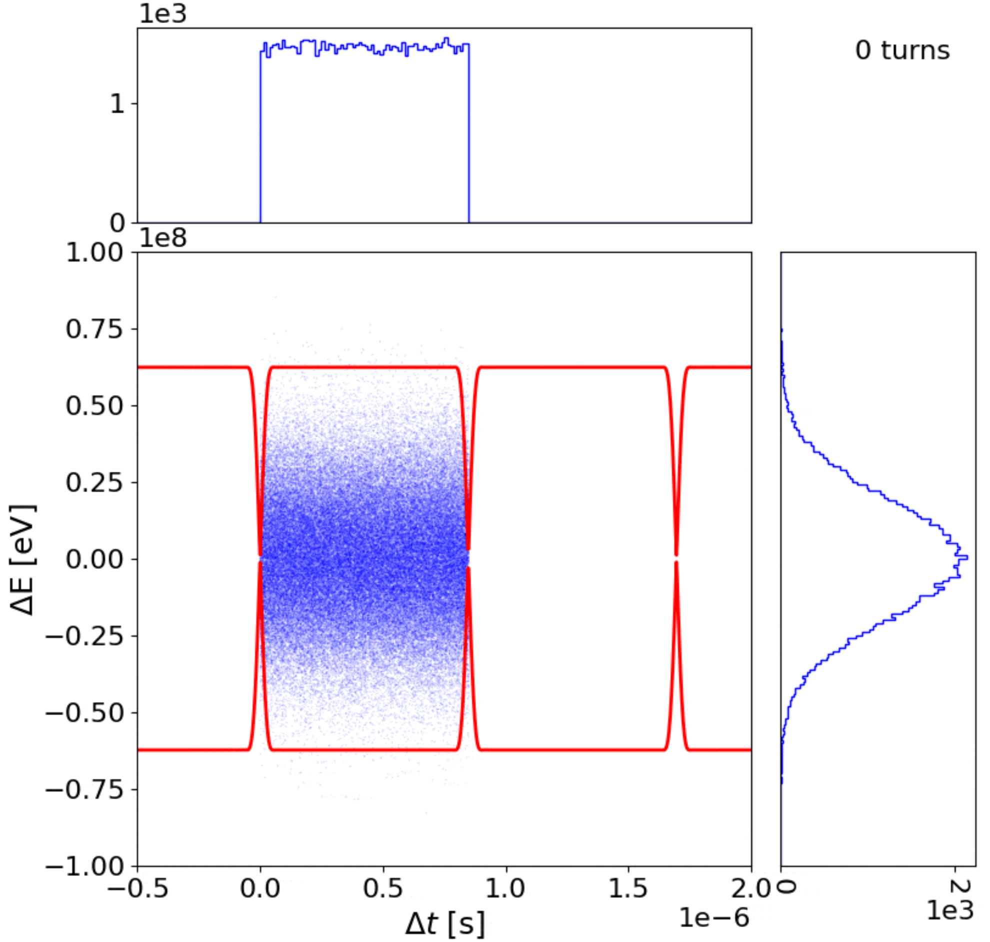

Space Charge Impedance Effect at Transition Jump

$$E_{kin}\left(n_{tr}-\frac{\Delta n_{jump}}{2}\right)=5.708\times10^{9}\ \text{eV}\quad \gamma\left(n_{tr}-\frac{\Delta n_{jump}}{2}\right)=7.086\quad p\left(n_{tr}-\frac{\Delta n_{jump}}{2}\right)=6.58\times10^{9}\quad E_{beam}\left(n_{tr}-\frac{\Delta n_{jump}}{2}\right)=6.646\times10^{9}$$

$$E_{kin}\left(n_{tr}+\frac{\Delta n_{jump}}{2}\right)=5.71\times10^{9}\ \text{eV}\quad \gamma\left(n_{tr}+\frac{\Delta n_{jump}}{2}\right)=7.088\quad p\left(n_{tr}+\frac{\Delta n_{jump}}{2}\right)=6.582\times10^{9}\quad E_{beam}\left(n_{tr}+\frac{\Delta n_{jump}}{2}\right)=6.648\times10^{9}$$

$$E_{kin}\left(n_{tr}+\frac{\Delta n_{jump}}{2}\right)-E_{kin}\left(n_{tr}-\frac{\Delta n_{jump}}{2}\right)=1.867\times10^{6}\ \text{eV (1.8 MeV in)}\quad 2\frac{\Delta n_{jump}}{2}=6.225\times10^{3}\ \text{turns}$$

- Jump – (3[d] stage)
- Only SC
- No RF
- $\alpha_{0,1,2}$ change at a turn

$$\Delta n_{jump}:=\frac{2\Delta\gamma_{tr}}{T_s\cdot d\gamma dt}=6.225\times10^{3}$$

$$T_s\cdot d\gamma dt\cdot\Delta n_{jump}=0.09$$

$$T_s\cdot\Delta n_{jump}\cdot10^{3}=10.588\ \text{ms}$$

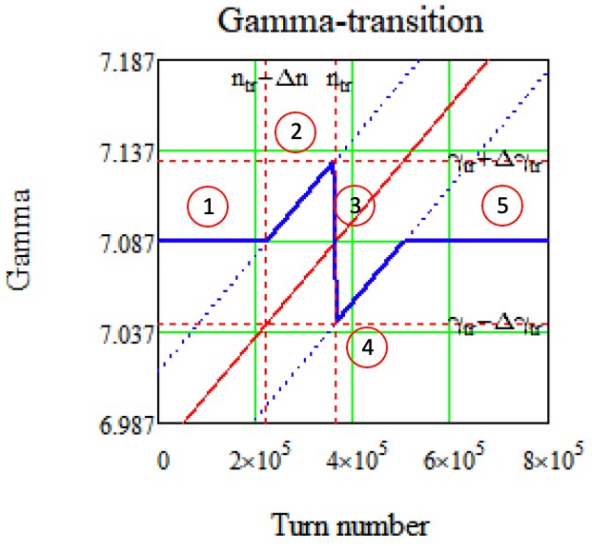

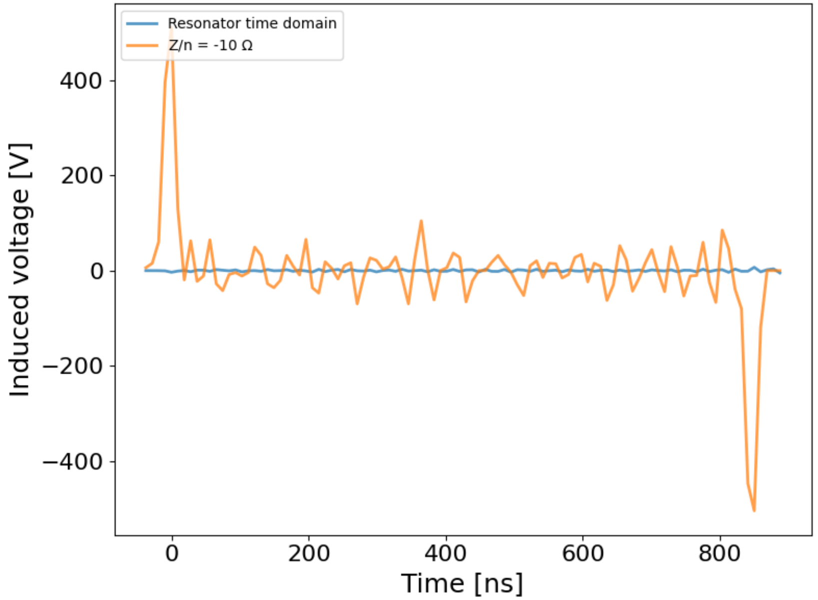

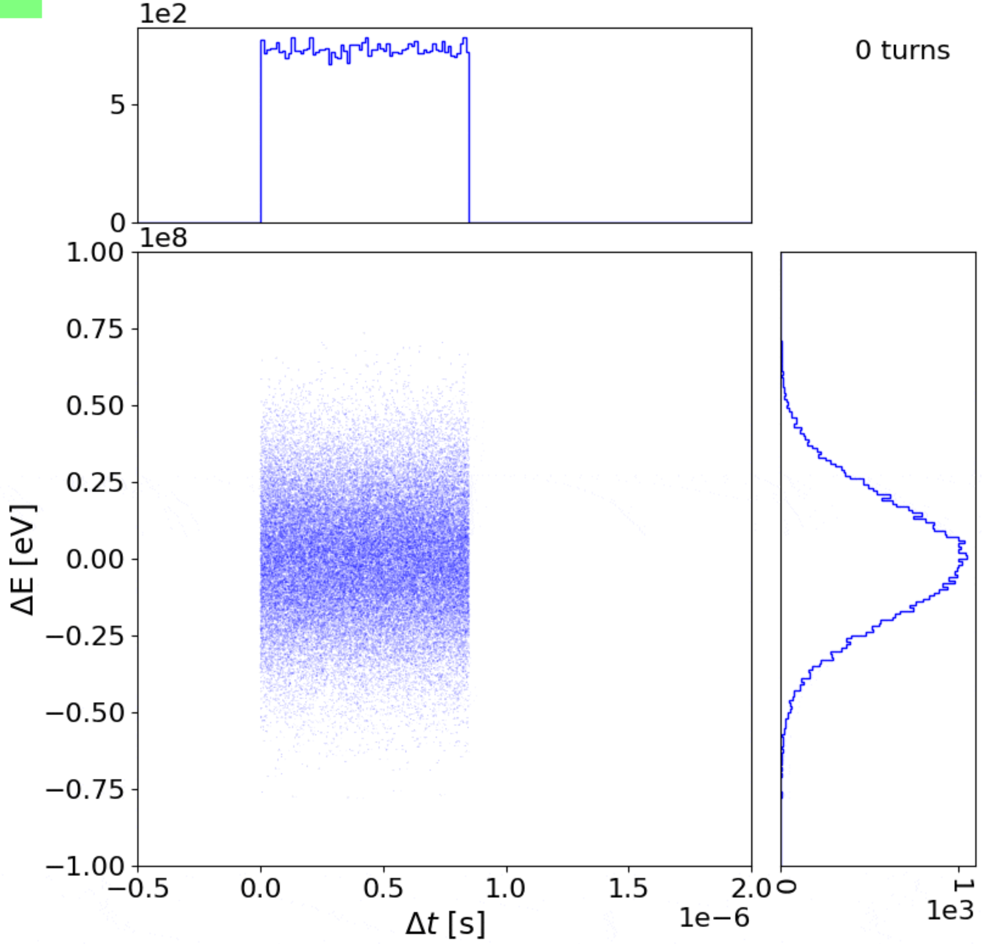

Spin Tracking

Particle Spin Tracking (Acceleration near Transition)

T-BMT Equations

$$\frac{d\vec{S}}{dt} = \vec{S}\times\vec{\Omega}_{MDM},$$

$$\vec{\Omega}_{MDM} = \frac{q}{m\gamma}\left\{(\gamma G + 1)\vec{B}_{\perp} + (G + 1)\vec{B}_{\parallel} - \left(\gamma G + \frac{\gamma}{\gamma + 1}\right)\frac{\vec{\beta}\times\vec{E}}{c}\right\}$$

⇓

$$\vec{\Omega}_{MDM} = \frac{q}{m\gamma}(\gamma G + 1)\vec{B}_{\perp}$$

<u>For pure magnetic ring</u>

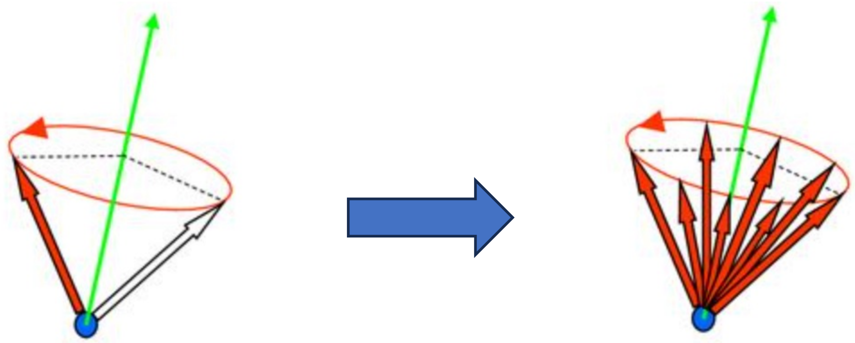

Particle Spin Tracking (Acceleration near Transition)

Parameters

Lattice:

$\gamma_p = 7.042$

$\gamma_{tr} = 7.087$

$\eta_0 = -1\times10^{-4}$

$turns = 2\times10^5$

Spin:

$\alpha_{YZ} = 45°$

RF is turn on

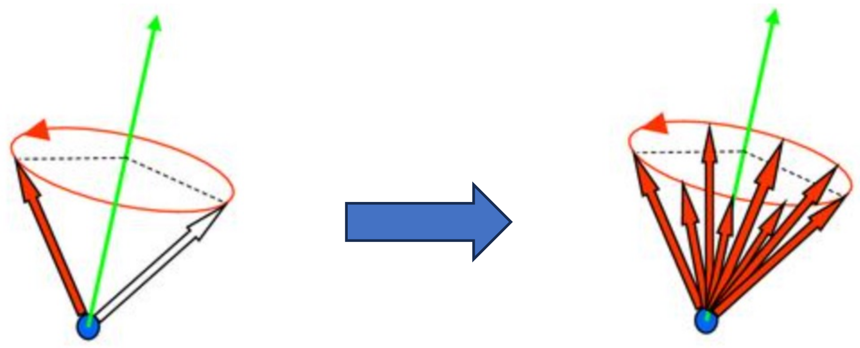

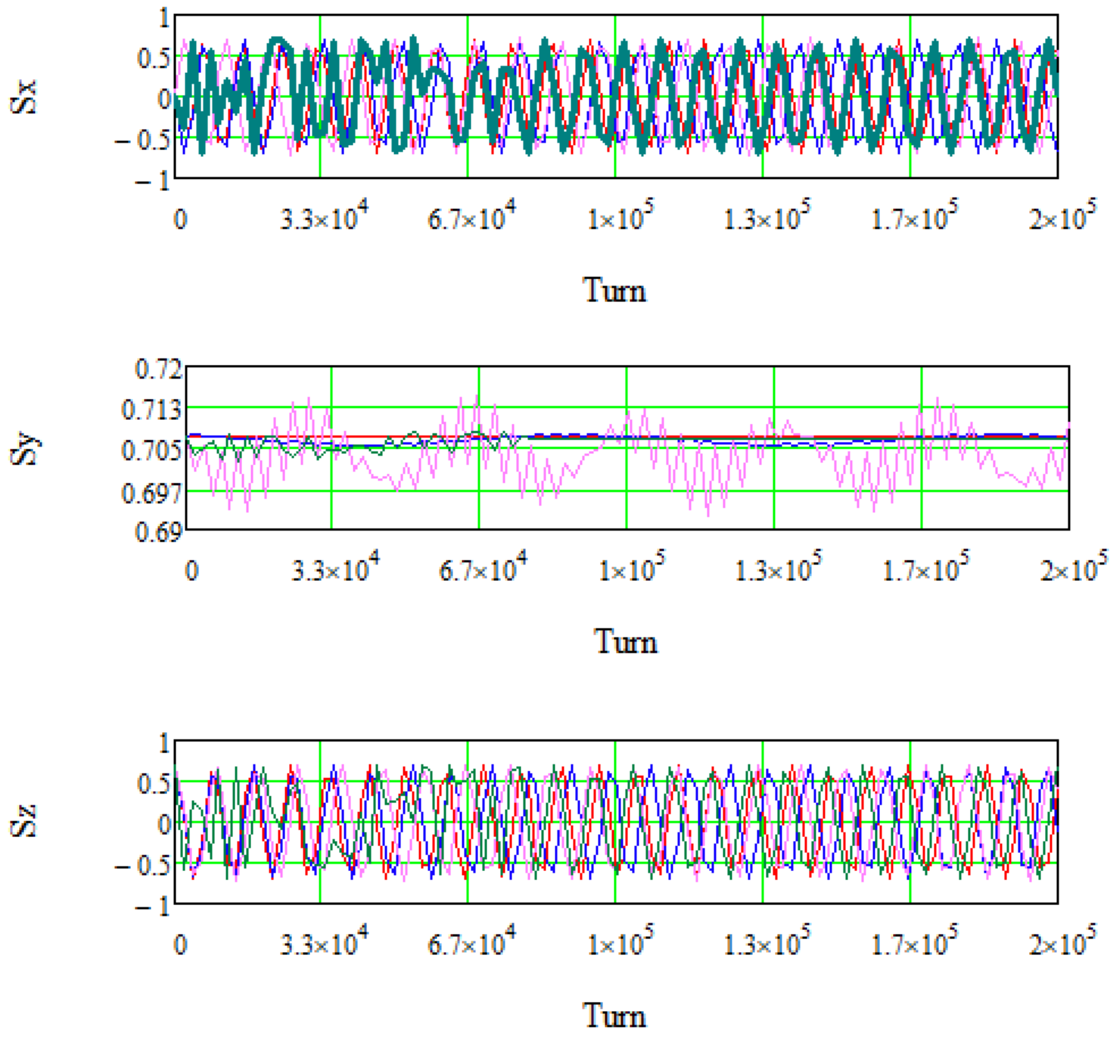

COSY Infinity: https://www.bmtdynamics.org/cosy/

Polarization (Acceleration near Transition)

Parameters

Lattice:

$\gamma_p = 7.042$

$\gamma_{tr} = 7.087$

$\eta_0 = -2\times10^{-4}$

$turns = 2\times10^5$

Spin:

$\alpha_{YZ} = 45°$

RF is turn on

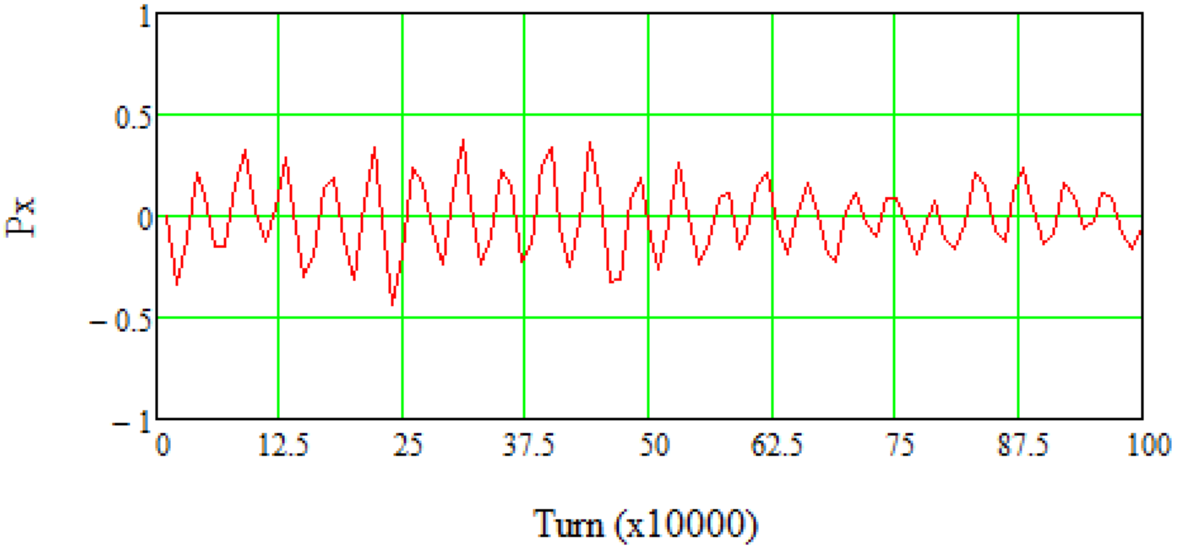

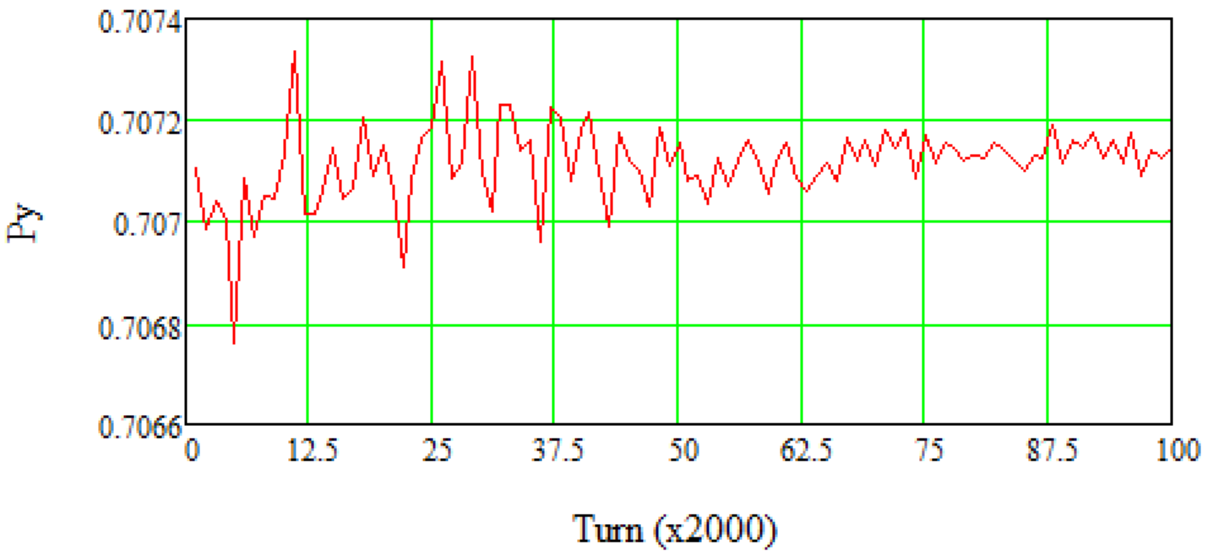

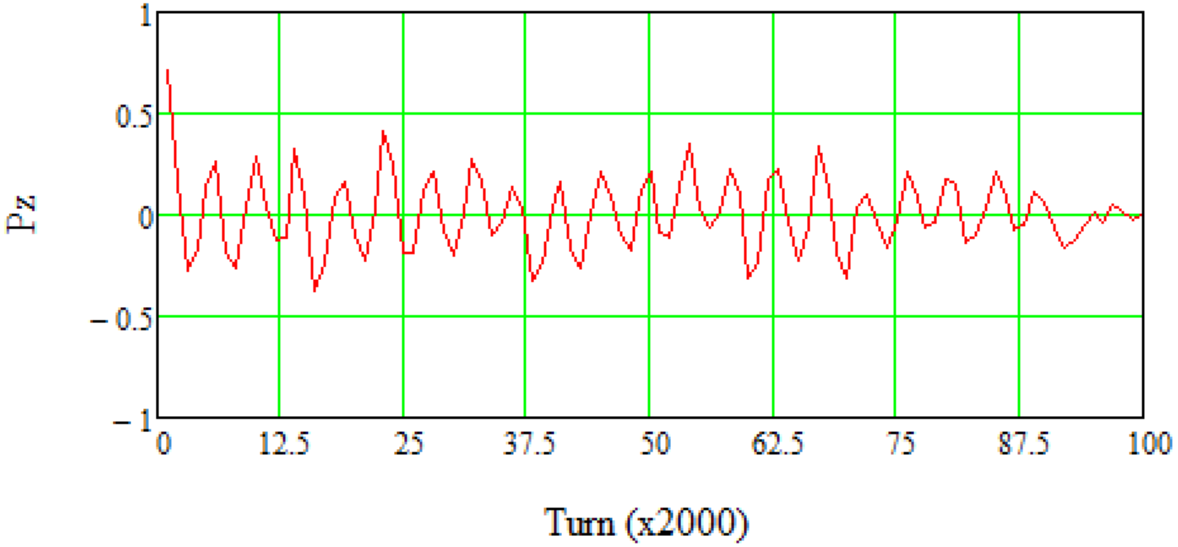

Lattice Parameters (during Jump)

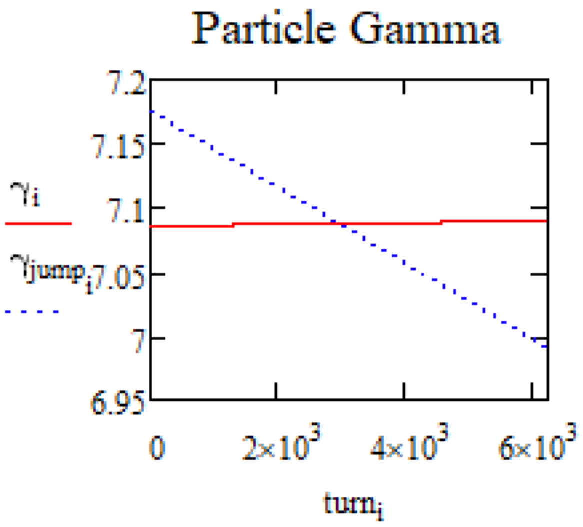

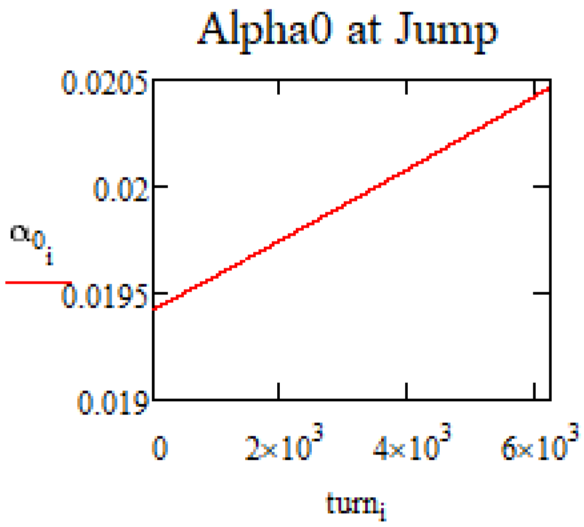

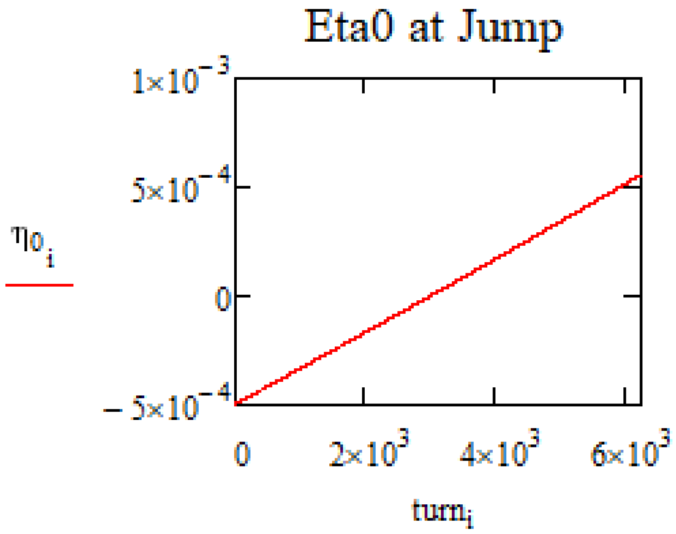

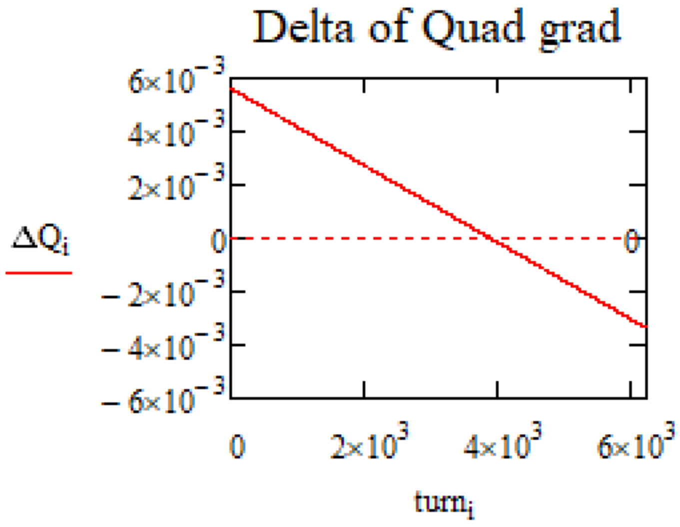

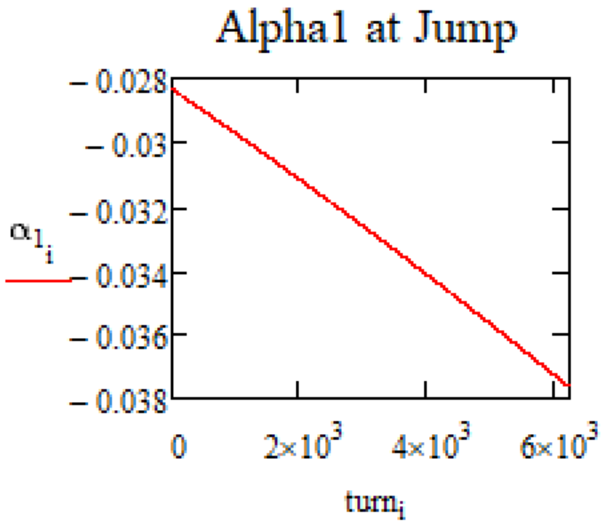

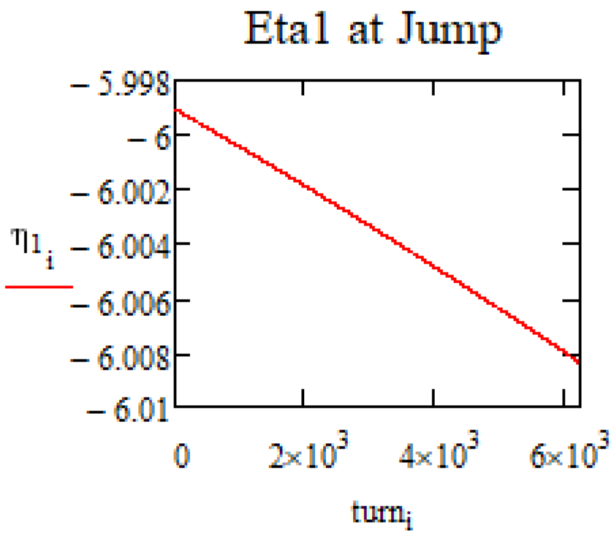

Particle Spin Tracking (during Jump)

Parameters

Lattice:

γ_p = from 7.0856 to 7.0896

γ_{tr} = from 7.1754 to 6.9903

Max($|\eta_0|$) $= 5\times10^{-4}$

$turns = 6225$

Spin:

$\alpha_{YZ} = 45°$

RF is turn off

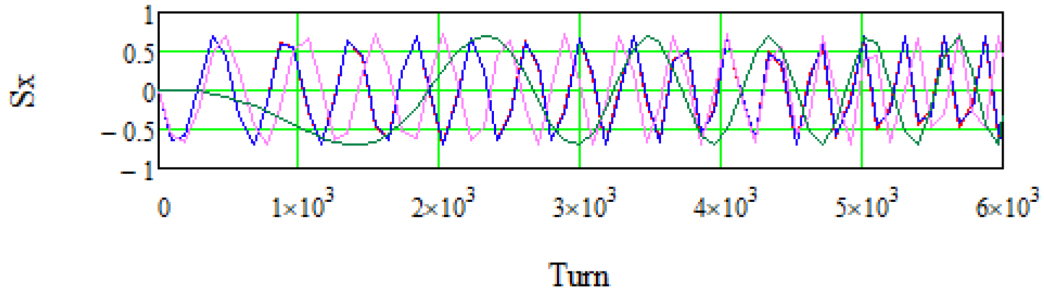

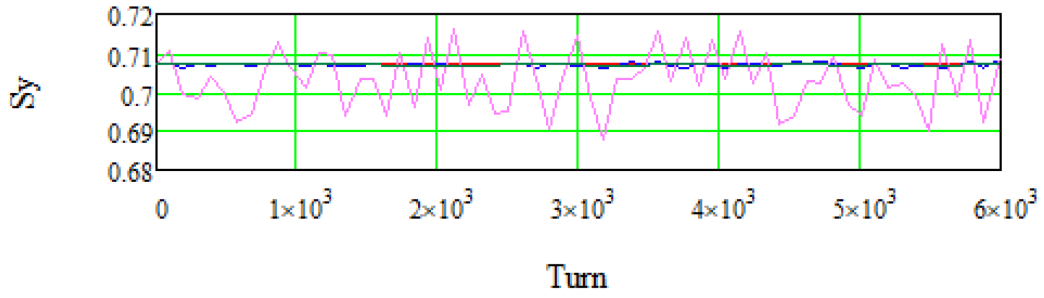

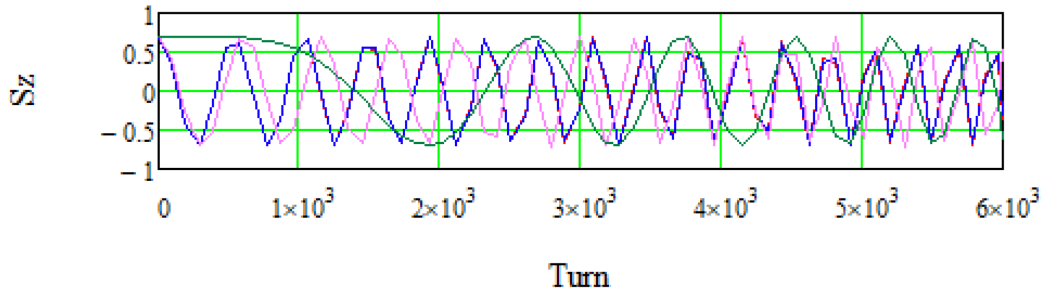

Shown 4 particles with different initial parameters in $x, y, {}^{dp}/_{p}$

Polarization (during Jump)

Parameters

Lattice:

γ_p = from 7.0856 to 7.0896

γ_{tr} = from 7.1754 to 6.9903

$\text{Max}(|\eta_0|) = 5\times10^{-4}$

$turns = 6225$

Spin:

$\alpha_{YZ} = 45°$

RF is turn off

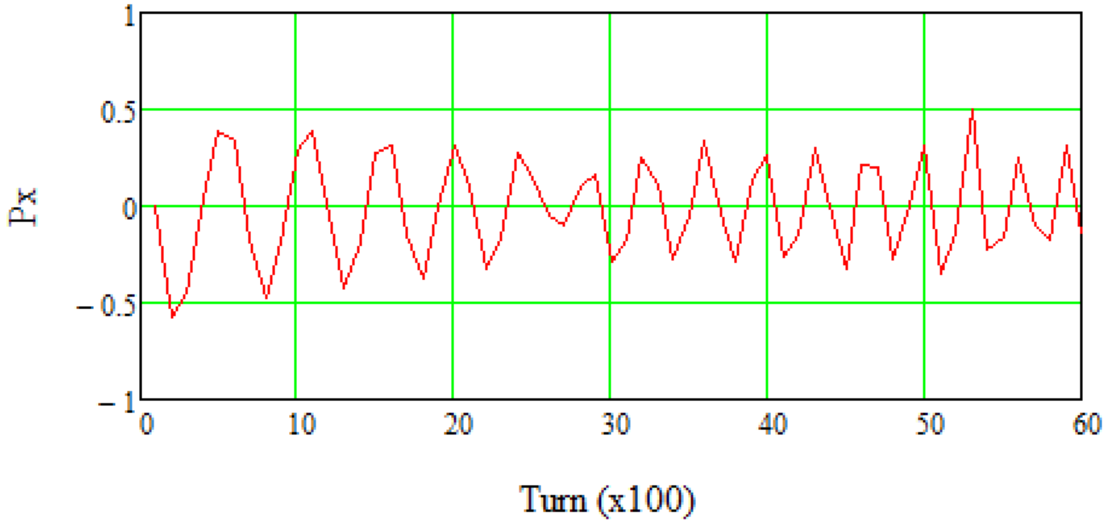

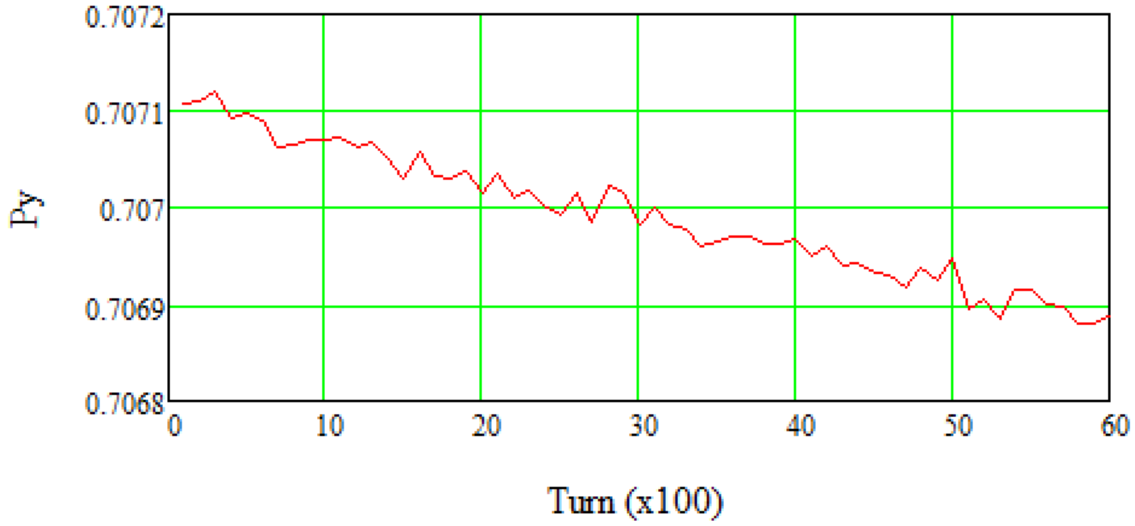

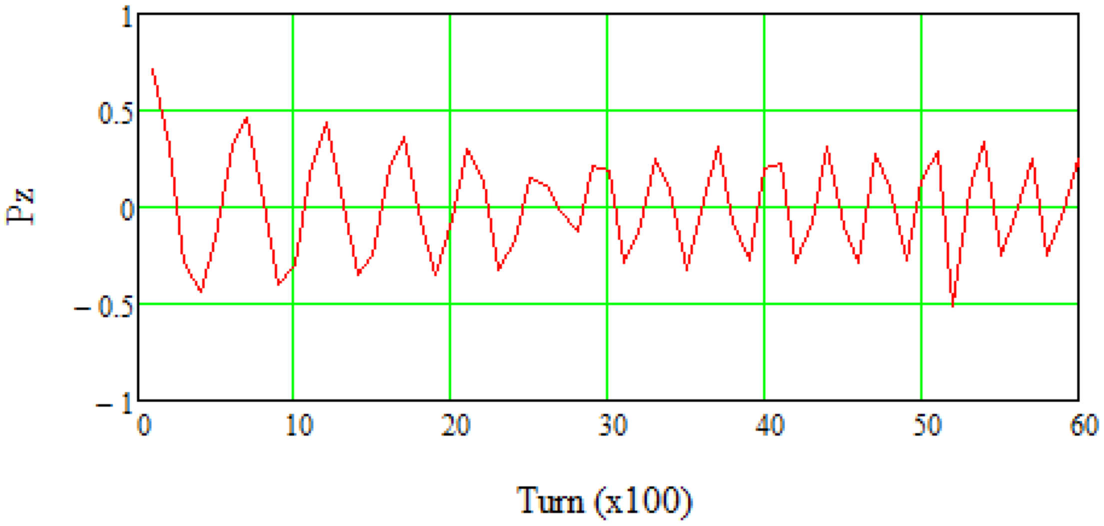

Conclusion

Considered:

- Longitudinal Dynamic Modeling
  near Transition Energy taking into account
  high orders of MCF and Impedances;
- Spin Tracking to consider polarization.

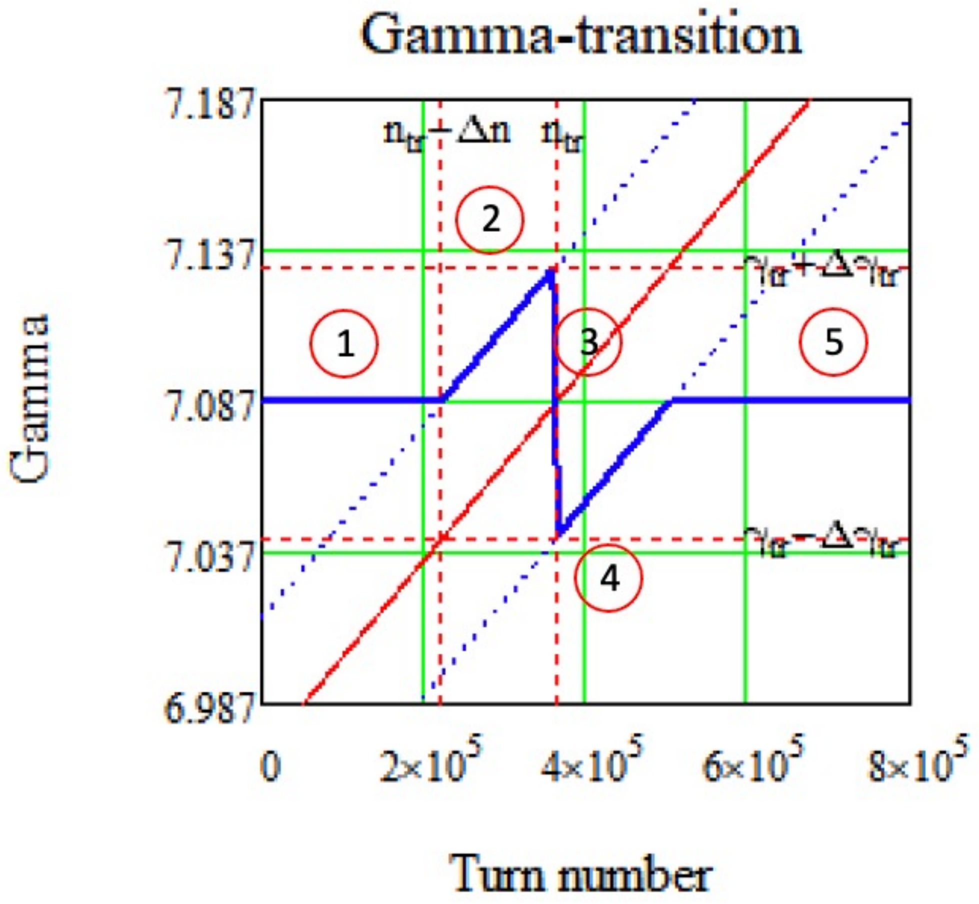

Outcomes:

- During the jump procedure the beam hold in separatrix;
- And the polarization is not destroyed;
- Transition Energy Jump is an available option cross transition energy.

References

1. Laclare, J L (ESRF, Grenoble), Coasting beam longitudinal coherent instabilities, CAS - CERN Accelerator School : 5th General Accelerator Physics Course, pp.349-384, DOI: 10.5170/CERN-1994-001.349
2. Jens Schweickhardt, Modeling and Optimization of Barrier-Bucket RF Systems, 2021
3. Mihaly Vadai, Beam Loss Reduction by Barrier Buckets in the CERN Accelerator Complex, CERN, Geneva, 2021
4. П.Р. Зенкевич, А.А. Коломиец, Электромагнитное моделирование элементов структуры коллайдера NICA, Письма в ЭЧАЯ. 2020. Т. 17, № 4(229). С. 445–452
5. A. Tribendis and others, Constraction and first test results of the barrier and harmonic RF systems for the NICA collider, IPAC2021, Campinas, SP, Brazil, doi:10.18429/JACoW-IPAC2021-MOPAB365
6. A.M. Malyshev and others, Barrier station RF1 of the NICA collider. Design features and influence on beam dynamics, RuPAC2021, Alushta, Russia, doi:10.18429/JACoW-RuPAC2021-WEPSC15
7. P. F. Derwent, Implementation of BLonD for Booster Simulations, Beams-doc # 8690, 2020
8. BLonD: https://blond.web.cern.ch/
9. COSY Infinity: https://www.bmtdynamics.org/cosy/

Backups

Barrier Bucket

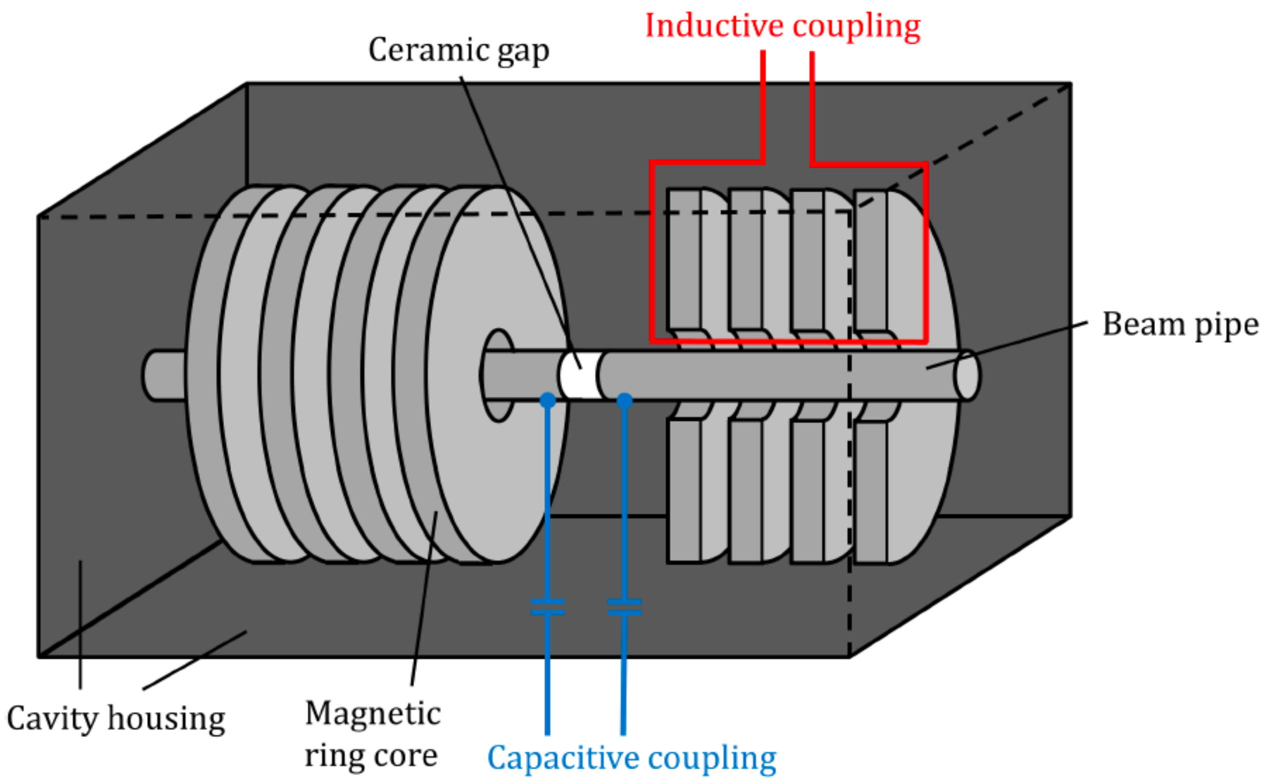

Figure 3.1: Simplified sketch of a cavity loaded with magnetic ring cores and one cavity gap. Two different coupling strategies to couple the cavity to the power amplifier stage are shown: capacitive coupling (blue), where the RF voltage is applied via coupling capacitors, and inductive coupling (red), where the signal is fed to the cavity via windings around the magnetic ring cores, comparable to a transformer.

Jens Schweickhardt, Modeling and Optimization of Barrier-Bucket RF Systems, 2021

Principle of stacking with BB

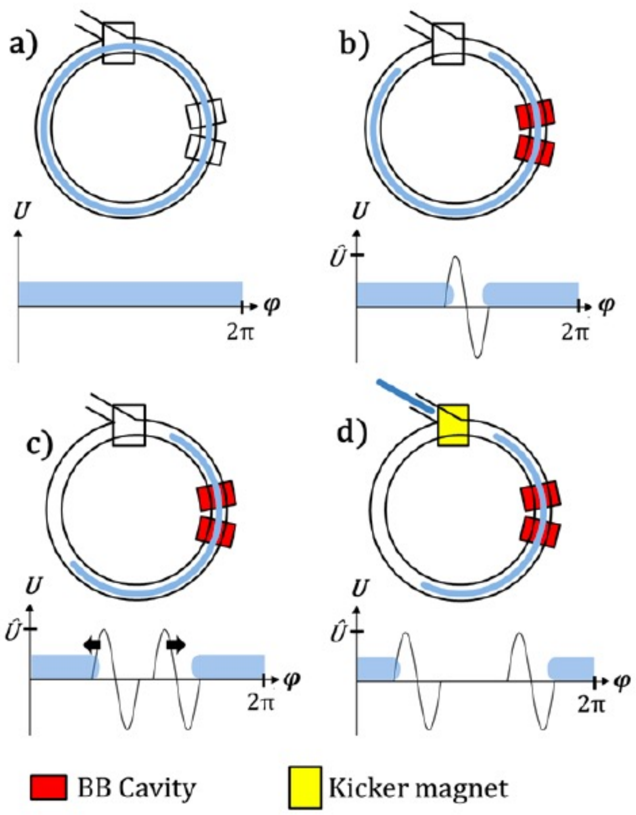

Figure 3.7: General principle of longitudinal stacking with sinusoidal BB pulses. Starting with a coasting beam (a), two BB pulses will be simultaneously ramped up by two BB systems, creating a gap in the beam due to the generated potential barrier (b). In the next step, the two pulses will be shifted apart, producing an empty bucket in-between (c). Once this bucket is large enough, a new bunch will be injected into the empty bucket (d). In the end, the BB pulses will be ramped down, enabling the particles to merge and to form a coasting beam again.

Jens Schweickhardt, Modeling and Optimization of Barrier-Bucket RF Systems, 2021

Barrier Bucket at NICA

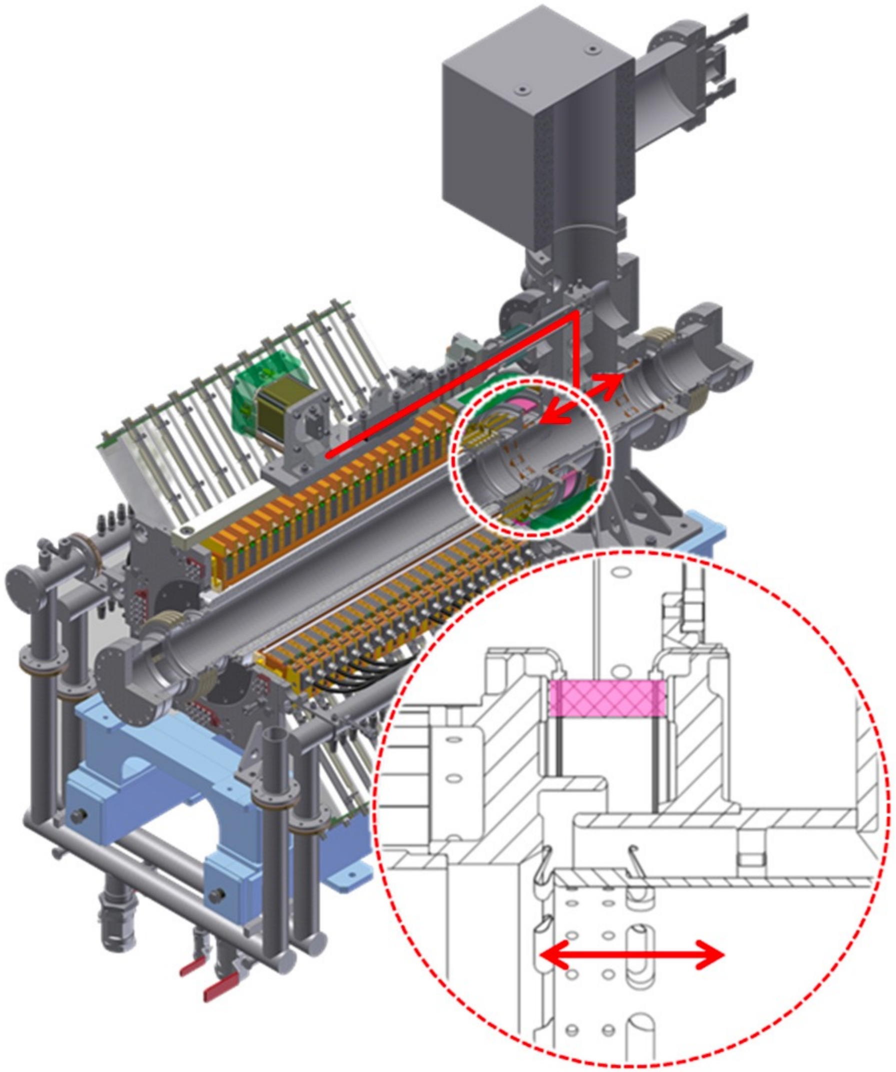

RF1 BARRIER BUCKET SYSTEM

RF1 is an induction accelerator composed by 20 inductor sections: 15 are used to form the barriers, 3 generate accelerating meander voltage and 2 passive damping sections correct voltage shape. Each active section is driven by a pair of pulse generators. An inductor section consists of a magnetic core made from the amorphous magnetic alloy Amet 84XB-M (82% Co) and glued between the 2 water cooled copper plates (heat exchangers). The total power

nique. RF1 also can accelerate the accumulated beam if the injection energy is lower than that of the experiment. Harmonic systems, RF2 and 3, are used to form 22 bunches with required parameters [2]. Each collider ring has one RF1 station, four RF2 and eight RF3 stations.

A. Tribendis and others, Constraction and first test results of the barrier and harmonic RF systems for the NICA collider, IPAC2021, Campinas, SP, Brazil, doi:10.18429/JACoW-IPAC2021-MOPAB365

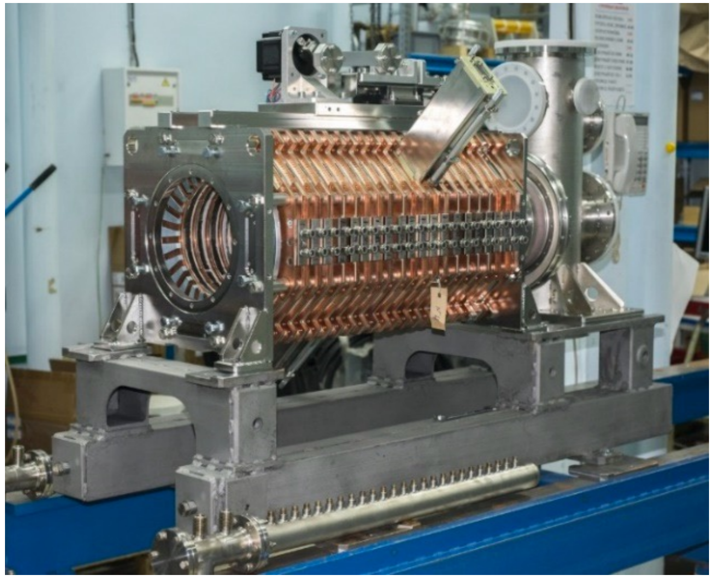

Barrier Bucket at NICA

The RF1 system generates 2 pairs of ±5 kV pulses (accelerating and decelerating in each pair) at the bunch revolution frequency thus forming the two separatrices – injection and stack. A bunch from the Nuclotron is shot into the injection separatrix, moved and added to the stack by switching off the pulses separating the two separatrices and so merging the two bunches. If the combined bunch length exceeds the half-ring perimeter it is compressed by moving the barrier pulses. Ion accumulation process is accomplished by the electron cooling. The accumulated ions trapped between the two barrier pulses may be accelerated, if needed, by ±0.3 kV meander voltage generated by the RF1 as well [2].

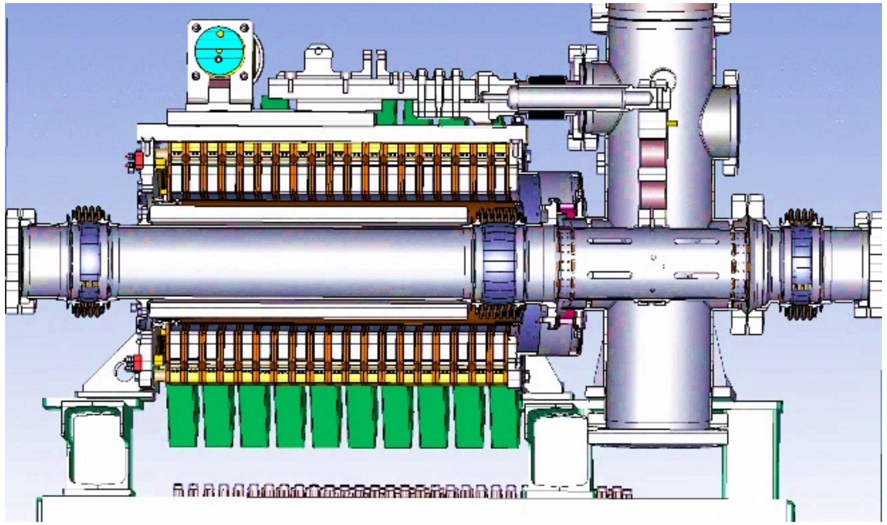

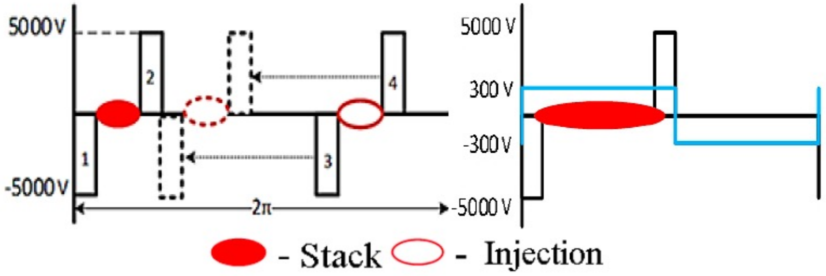

Figure 3: Barrier voltage (left) and acceleration (right).

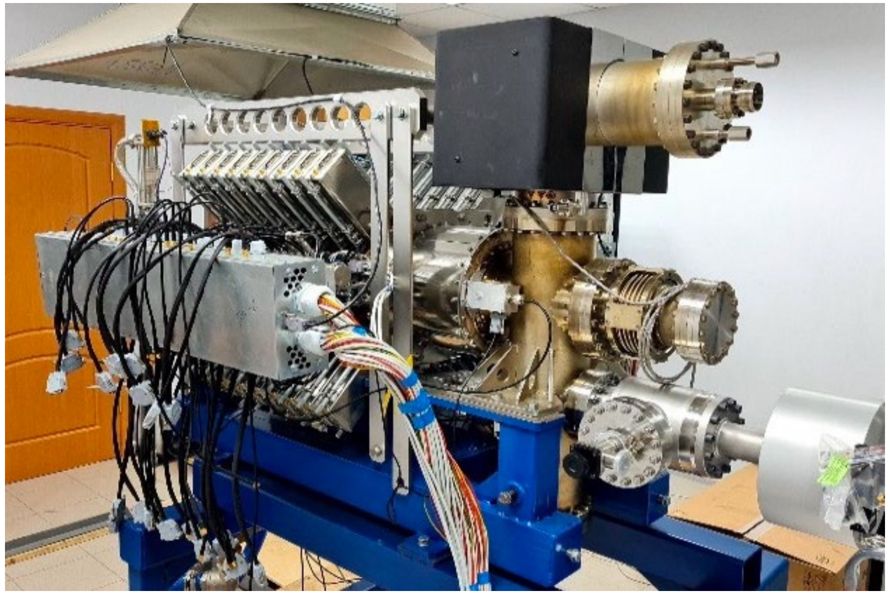

A.M. Malyshev and others, Barrier station RF1 of the NICA collider. Design features and influence on beam dynamics, RuPAC2021, Alushta, Russia, doi:10.18429/JACoW-RuPAC2021-WEPSC15

BB RF1 Impedances

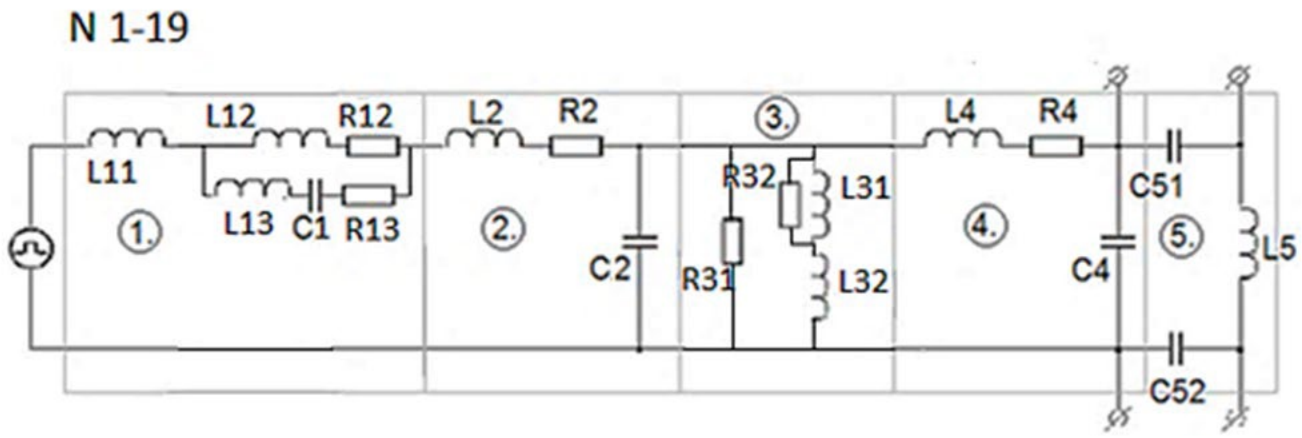

Equivalent circuit of one ring (from the 1st to the 19th).

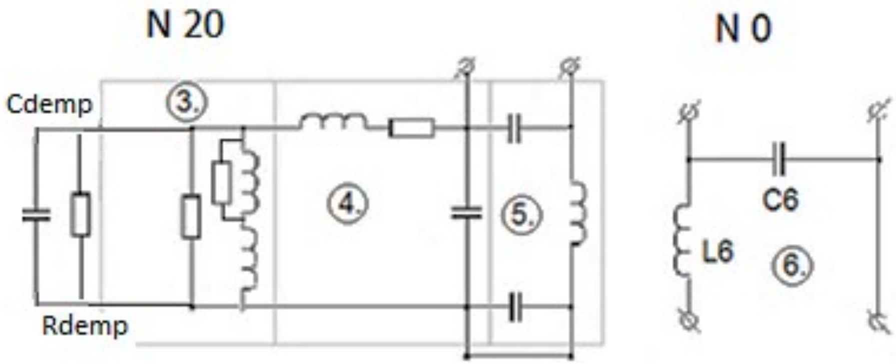

Last ring and accelerating gap.

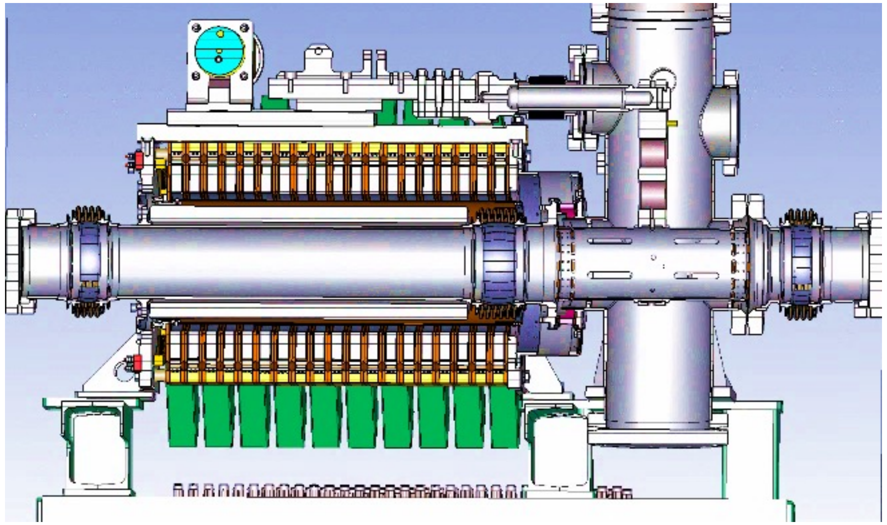

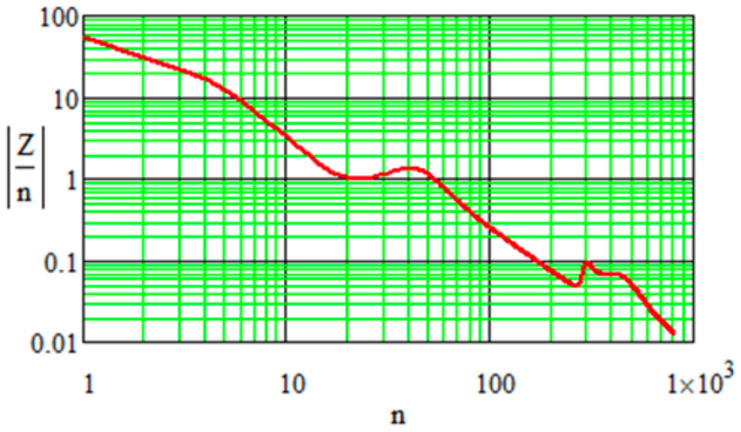

System impedance calculated by equivalent circuit impedance

A.M. Malyshev and others, Barrier station RF1 of the NICA collider. Design features and influence on beam dynamics, RuPAC2021, Alushta, Russia, doi:10.18429/JACoW-RuPAC2021-WEPSC15

BB RF1 Impedances

Microwave Instability

A table of threshold values of the beam current at energies from 1 to 4.5 GeV/u was calculated (Table 1, φbb = 10/12π).

$$I_0 \le \varphi_{bb} \frac{(A_{Au}E / Z_{Au}e)|\eta|\delta_{p\,av}^{\ 2}}{|Z_{out}(n\omega_0)/n|_{\max}}$$

RF1 impedance (max 60ohm, see Fig. 10) at 0.4A does not cause microwave instability.

Table 1: Microwave Instability Threshold

Energy, GeV/u	**1**	**3**	**4.5**
$\Delta p_{sep}/3$, 10^{-3}	0.24	0.37	0.6
Threshold current, A, at $|Z/n|_{\max} = 60\,Ohm$	2.6A	2.2A	0.8A

A.M. Malyshev and others, Barrier station RF1 of the NICA collider. Design features and influence on beam dynamics, RuPAC2021, Alushta, Russia, doi:10.18429/JACoW-RuPAC2021-WEPSC15

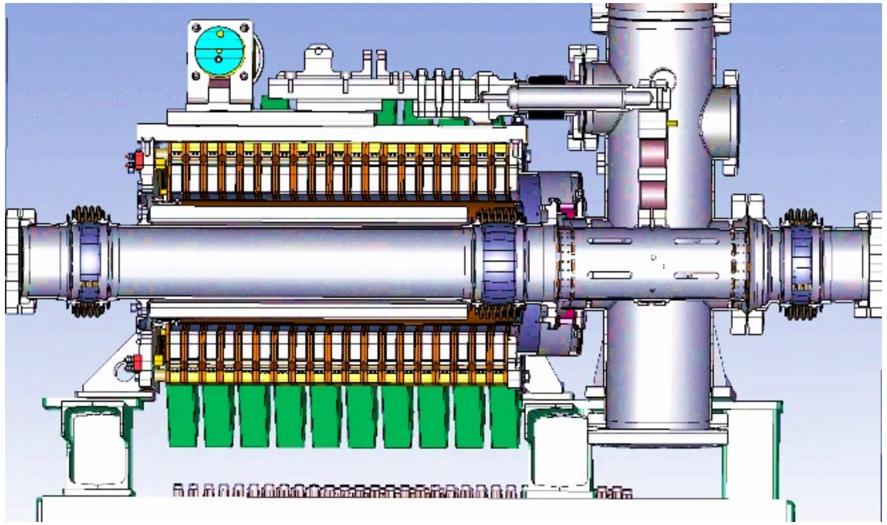

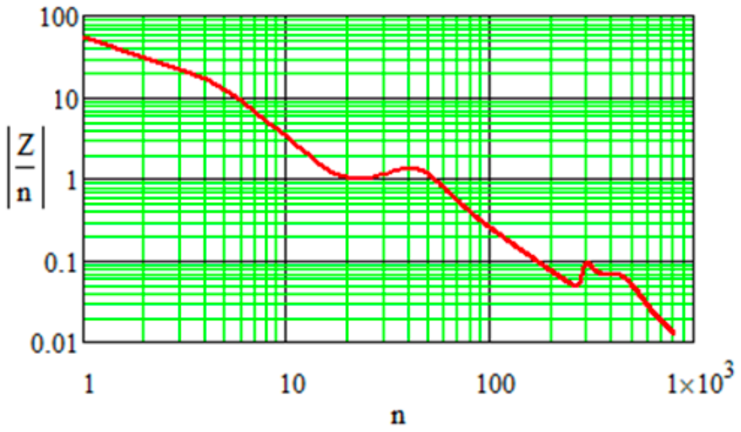

System impedance calculated by equivalent circuit impedance

Dispersion Relation

– distribution function: $\Psi(\tau,\dot{\tau},t) = g_0(\dot{\tau}) + g_p(\dot{\tau}) \exp j(p\omega_0\tau + \omega_{//pc}t)$ (77)

– perturbation signal: $S_{//p}(t,\theta) = IT_0 \exp j[(p\omega_0+\omega_{//pc})t-p\theta] \int_{\dot{\tau}} g_p(\dot{\tau})d\dot{\tau}$ (78)

– the general impedance of a ring $Z_{//}$,

– the general expression of the EM field generated by a signal in a ring with impedance $Z_{//}$

$$[\vec{E}+\vec{v}\times\vec{B}]_{//}(t,\theta) = \frac{-1}{2\pi R}\int_{\omega=-\infty}^{\omega=+\infty} Z_{//}(\omega)\, S_{//}(\omega,\theta) \exp j\omega t\, d\omega \quad (79)$$

– The EM force acts back on the particles,

$$\ddot{\tau} = \frac{\eta}{p_{//0}}\frac{dp_{//}}{dt} = \frac{\eta e}{p_{//0}}[\vec{E}+\vec{v}\times\vec{B}]_{//}(t,\theta) \quad (82)$$

Laclare, J L (ESRF, Grenoble), Coasting beam longitudinal coherent instabilities, CAS - CERN Accelerator School : 5th General Accelerator Physics Course, pp.349-384, DOI: 10.5170/CERN-1994-001.349

Vlasov's Equation and Dispersion Relation

$$\frac{\partial\Psi}{\partial t} + \vec{v}\ \overrightarrow{\text{grad}\Psi} = 0$$

$$\frac{\partial\Psi}{\partial t} + \frac{\partial\Psi}{\partial\tau}\dot{\tau} + \frac{\partial\Psi}{\partial\dot{\tau}}\ddot{\tau} = \frac{d\Psi}{dt} = 0 \qquad (89)$$

In this form, it is called Vlasov's equation.

will be drawn is called the Dispersion Relation. It is independent of g_p . In other words, the growth rate of the instability is independent of the exact form of g_p .

$$1 = \frac{\eta(\frac{q}{A})I}{(\frac{m_0c^2}{e})\gamma_0\beta_0^2}\ j\ \frac{Z_{//}(\Omega_c)}{p\omega_0}\int\frac{\frac{\partial g_0}{\partial\dot{\tau}}}{\frac{\omega_{//}pc}{p\omega_0}+\dot{\tau}}\,d\dot{\tau} \qquad (94)$$

Laclare, J L (ESRF, Grenoble), Coasting beam longitudinal coherent instabilities, CAS - CERN Accelerator School : 5th General Accelerator Physics Course, pp.349-384, DOI: 10.5170/CERN-1994-001.349